Journal of South American Earth Sciences 79 (2017) 67–94

Contents lists available at ScienceDirect

Journal of South American Earth Sciences

journal homepage: www.elsevier.com/locate/jsames

# The Sanrafaelic remagnetization revisited: Magnetic properties and magnetofabrics of Cambrian-Ordovician carbonates of the Eastern Precordillera of San Juan, Argentina

Sabrina Y. Fazzito [a, c, *], Augusto E. Rapalini [a, c], Daniel G. Poiré [b, c]

[a] Universidad de Buenos Aires, Laboratorio de Paleomagnetismo Daniel A. Valencio, Instituto de Geociencias Básicas, Aplicadas y Ambientales de Buenos Aires (IGEBA), Departamento de Ciencias Geológicas, Facultad de Ciencias Exactas y Naturales, Intendente Güiraldes 2160, Pabellón II, Ciudad Universitaria, C1428EGA, Buenos Aires, Argentina
[b] Centro de Investigaciones Geológicas (CIG), Diagonal 113 N°275, 1900, La Plata, Argentina
[c] Consejo Nacional de Investigaciones Científicas y Técnicas (CONICET), Argentina

ARTICLE INFO

*Article history:*
Received 10 December 2016
Received in revised form
7 July 2017
Accepted 24 July 2017
Available online 27 July 2017

*Keywords:*
Remagnetized carbonates
Sanrafaelic remagnetization
Magnetic fabrics
Eastern precordillera
Cuyania terrane
Argentina

ABSTRACT

Systematic rock-magnetic and magnetofabric studies were carried out on samples from twenty-three palaeomagnetic sites distributed on the La Laja, Zonda, La Flecha, La Silla and San Juan Formations, which constitute a thick middle Cambrian to early Ordovician carbonate sequence exposed in the Eastern Precordillera of Argentina. Previous palaeomagnetic studies on these rocks showed that this succession is characterized by a recent full overprint in the lower levels and a post-tectonic Permian remagnetization associated to the widespread Sanrafaelic event in the upper part. Our investigation revealed that the fluctuations of the magnetic properties are stratigraphically (lithologically) controlled. Anisotropy of magnetic and anhysteretic susceptibility measurements defined consistent fabrics along the entire section that switch progressively from "inverse", at the bottom, to "normal", at the top, with "intermediate" fabrics occurring mainly at medium levels. Degree of dolomitization significantly affects many rock-magnetic parameters, but appears unrelated to the presence of the Permian remagnetization, which is determined to reside in magnetite despite the complex magnetic mineralogy shown by the studied carbonates. Hysteresis cycles of rocks affected by the Sanrafaelic remagnetization are governed by ferromagnetic fractions showing a clear difference respect to those not affected and characterized by the dominance of paramagnetic or diamagnetic signals. The magnetic fabrics and mineralogical characterization rule out a thermoviscous origin and suggest a chemical remagnetization originated in the authigenic formation of magnetite for the Sanrafaelic overprint. X-ray diffraction analyses indicate that clay minerals are virtually absent in the whole succession with no traces of illite in any sample, discarding burial diagenesis of clay minerals for the origin of the remagnetization. Lack of late Palaeozoic magmatic rocks near the study area difficults correlation of this event with hydrothermal brines as well as casts serious doubts on any effect produced by an assumed geothermal anomaly associated with the Permo-Triassic Choiyoi magmatic province. The original model of remagnetization associated to chemically active fluids expelled from the San Rafael Orogen towards the foreland still holds as a viable mechanism.



## 1. Introduction

The importance of the widespread Sanrafaelic remagnetization event, which produced the resetting of most of the early Cambrian to mid-Ordovician carbonate platform of the Argentine Precordillera and calcareous units of the San Rafael Block, lies in the restrictions it poses on the palaeogeographic reconstruction of the Laurentian-derived Cuyania terrane (Astini et al., 1995; Ramos,

* Corresponding author. Universidad de Buenos Aires, Laboratorio de Paleomagnetismo Daniel A. Valencio, Instituto de Geociencias Básicas, Aplicadas y Ambientales de Buenos Aires (IGEBA), Departamento de Ciencias Geológicas, Facultad de Ciencias Exactas y Naturales, Intendente Güiraldes 2160, Pabellón II, Ciudad Universitaria, C1428EGA, Buenos Aires, Argentina.
*E-mail addresses:* sabrinafazzito@gl.fcen.uba.ar (S.Y. Fazzito), rapalini@gl.fcen.uba.ar (A.E. Rapalini), poire@cig.museo.unlp.edu.ar (D.G. Poiré).

http://dx.doi.org/10.1016/j.jsames.2017.07.010
0895-9811/

2004; Rapalini, 2012) during the early Palaeozoic and in the interest in elucidating the processes that triggered regional remagnetizations (e.g. Font et al., 2012).

Previous palaeomagnetic studies (Rapalini and Astini, 2005, and references therein) have evidenced a migration pattern of the Sanrafaelic remagnetization front, in which the geologic units of the Western Precordillera suffered a magnetic overprint during the early Permian, while those in the Eastern Precordillera were remagnetized during the late Permian. This has been interpreted as caused by an eastward migration of fluids expelled from the orogenic area (Rapalini and Astini, 2005) associated to the San Rafael tectonic event (Azcuy and Caminos, 1987; Ramos and Folguera, 2009; among many others). The particular spatial distribution of units affected by the pervasive overprint also led Rapalini and Astini (2005) to suggest that the Sanrafaelic remagnetization was conditioned by the different lithologies, i.e. while some units appeared completely remagnetized, others still carry the primary remanence and others show neither of them. Four different geologic units from the Precordillera and one from the San Rafael Block were recognized as non-remagnetized (Rapalini and Astini, 2005, and references there in). Among them, the early Cambrian Cerro Totora Formation, in the Precordillera of La Rioja (Rapalini and Astini, 1998), and the mid-Ordovician Pavón Formation, in the San Rafael Block (Rapalini and Cingolani, 2004), outstand for carrying primary magnetizations which are, up to now, the only palaeomagnetic constraints on the palaeogeographic evolution of the allochthonous (Laurentian) Cuyania terrane in the early Palaeozoic (Rapalini, 2012). On the other hand, palaeopoles from five units from Precordillera and one unit from the San Rafael Block, showed evidence of a Permian remagnetization that was associated with the San Rafaelic overprint (Rapalini and Astini, 2005). Fazzito and Rapalini (2016) have recently reported a detailed rock-magnetic study on the Middle Ordovician limestones of the Ponón Trehué Formation, exposed in the San Rafael Block. This study demonstrated a complex magnetic mineralogy carried by these rocks and a chemical origin coetaneous with folding for pyrrhotite and magnetite, both carriers of the late Palaeozoic syntectonic magnetization. However, this study was focused on a small-scale fold and despite the progress it produced in the knowledge of the Sanrafaelic remagnetization, its extrapolation to other units in the Argentine Precordillera is not straightforward. Further systematic studies on rock magnetic properties in a broader scale are needed for a better characterization of this widespread geologic process.

In this paper, we report a detailed rock-magnetic study on samples collected by Rapalini et al. (2000) along a nearly continuous middle Cambrian–early Ordovician carbonate sequence (limestones to dolomites) including the La Laja, Zonda, La Flecha, La Silla and San Juan Formations (Fig. 1) exposed in the Eastern Precordillera of Argentina. A recent magnetization, either as a partial overprint or as the single magnetic component appears in all lithologic types, while a post-folding overprint assigned to the Sanrafaelic regional remagnetization of Permian age was observed in the La Flecha, La Silla and San Juan Formations (Rapalini et al., 2000). The main goal of this study is to characterize the magnetic fingerprint of each of the different lithologies and to shed light on the origin and mechanisms of this regional geologic event. The ferromagnetic mineralogy and magnetic fabric (anisotropy of magnetic susceptibility and anisotropy of anhysteretic remanence) were determined and evaluated regarding the magnetic components of the remagnetization for each geologic unit. The rock magnetic proxies regarded as worldwide diagnostic properties of secondary magnetization in carbonates were also investigated.

## 2. Geologic background and stratigraphy

The Argentine Precordillera (Fig. 1) and the San Rafael Block, in central western Argentina, are part of the Cuyania composite terrane (Ramos, 1995, 2004), which is interpreted as an exotic Laurentian block that was accreted to Gondwana in the middle to late Ordovician (Astini et al., 1995). The Argentine Precordillera is characterized by a thick Cambrian-Middle Ordovician carbonate platform with well-dated fossil-rich assemblages and a basement of Grenvillian age (Astini et al., 1996; Ramos et al., 1998; Thomas et al., 2000; Ramos, 2004; among many others). This morphostructural unit is a north-south trending thrust-and-fold belt that extends about 80 km wide and 400 km long, uplifted during the Andean orogeny in the Neogene (Jordan et al., 1983; Zapata and Allmendinger, 1996). It is subdivided into three sections: Eastern, Central and Western Precordillera (Ortiz and Zambrano, 1981). Whereas the latter two are characterized by east-verging thin-skinned thrusts, the Eastern Precordillera is characterized by west-verging thick-skinned backthrusts (e.g. von Gosen, 1992; Milana and Zambrano, 1996; Vergés et al., 2007, and many others).

The palaeomagnetic study of Rapalini et al. (2000; Fig. 1) comprised 23 sites gathered from five middle Cambrian to early Ordovician carbonate units (a continuous succession of limestones to dolomites, Table 1) of the Eastern Precordillera: i) the La Laja Formation, which covers the upper Lower Cambrian to upper Middle Cambrian, has a maximum thickness of 1000 m and is mainly composed of subtidal mudstones and wackstones; ii) the Zonda Formation, which consists of ~300 m of dolomites and calcareous dolomites up to lower Upper Cambrian age; iii) the Upper Cambrian La Flecha Formation, made up of 500 m of limestones and dolomites; iv) the La Silla Formation, which encompasses the Cambrian-Ordovician boundary and consists of limestones with a few intercalated dolomitic levels and 350 m of maximum thickness and v) the San Juan Formation, which is composed of 300 m of massive grey limestones and marls of early Ordovician age. Detailed biostratigraphic studies of these units can be found in Bordonaro (1980, 2003a, b), Baldis and Bordonaro (1981, 1984), Baldis et al. (1982, 1984), Keller et al. (1994), Astini et al. (1995), Benedetto et al. (1995), Benedetto (2004), Gómez and Astini (2005), among others.

## 3. General results from previous palaeomagnetic studies

None of the 23 sampled sites from the carbonate sequence exhibited evidence of a primary remanence (Rapalini et al., 2000). Regarding their natural remanent magnetization (NRM), the study sequence can be subdivided into a lower section (La Laja and Zonda Formations, sites JS1 to JS10, localities 1 and 2 of Fig. 1a) with a single postectonic magnetization of exclusive normal polarity coincident with the Earth's dipole direction, and an upper one (La Flecha, La Silla and San Juan Formations, sites JS11 to JS23, localities 3, 4 and 5 of Fig. 1a) in which the carbonates show the presence of a dominantly reversed polarity magnetization interpreted of Permian age (Rapalini et al., 2000) with a partial overprint of a recent magnetization coincident with that found in the lower section units. A brief account of the NRM characteristics of both sections as described by Rapalini et al. (2000) follows. Each of the demagnetized specimens from the La Laja and Zonda Formations

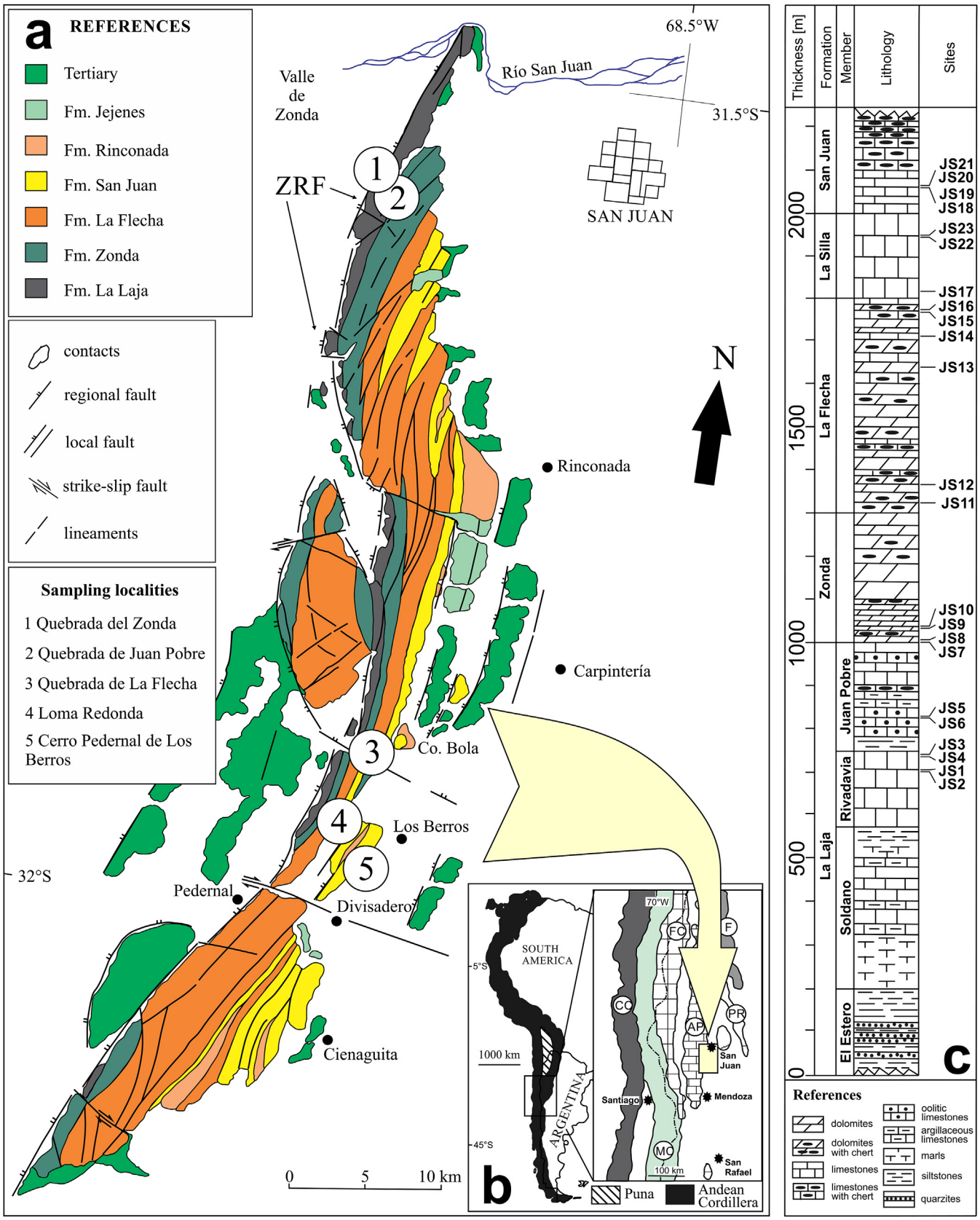


**Fig. 1.** **a)** The five palaeomagnetic sampling localities are identified by numbers on the geologic map of Sierra Chica de Zonda and Cerro Pedernal, Eastern Precordillera. Modified from Baldis and Bordonaro (1984) and Rapalini et al. (2000). ZRF: Zonda regional fault. **b)** Location map of the Argentine Precordillera. CC: Coastal Cordillera; MC: Main Cordillera; FC: Frontal Cordillera; AP: Argentine Precordillera; PR: Pampean Ranges; F: Famatina. **c)** Stratigraphic distribution of palaeomagnetic sites gathered from the La Laja, Zonda, La Flecha, La Silla and San Juan Formations. Modified from Baldis and Bordonaro (1984) and Rapalini et al. (2000).

**Table 1**
Lithology of the sampled carbonates from the Eastern Precordillera. Geologic formations, sites and stratigraphic height are indicated.

| Formation | Site | Height [m] | Lithology |
|---|---|---|---|
| La Laja | JS2 | 700 | |
| | JS1 | 703 | Well-stratified dark grey limestones with some calcite veins |
| | JS4 | 709 | |
| | JS3 | 712 | |
| | JS6 | 825 | Medium to dark grey oolitic limestones with several intercalations of yellowish-brown marlstones |
| | JS5 | 829 | |
| Zonda | JS7 | 1000 | Grey dolostones with chert |
| | JS8 | 1004 | |
| | JS9 | 1025 | Fine-grained laminated grey dolostones |
| | JS10 | 1030 | |
| La Flecha | JS11 | 1325 | Grey dolostones |
| | JS12 | 1360 | |
| | JS13 | 1640 | Homogeneous dark grey limestone |
| | JS14 | 1715 | |
| | JS15 | 1775 | Massive grey limestones |
| | JS16 | 1785 | |
| La Silla | JS17 | 1815 | |
| | JS22 | 1950 | Grey limestone, in part laminated (dolostones) |
| | JS23 | 1955 | |
| San Juan | JS18 | 2060 | |
| | JS19 | 2060 | Grey limestones with many calcite veins |
| | JS20 | 2063 | |
| | JS21 | 2063 | |

showed a single component of magnetization (Component A) trending towards the origin of coordinates (Fig. 2). This was in most cases completely erased by 400–500 °C during thermal demagnetization of the NRM (e.g. samples JS1-3b, JS5-6b, JS7-3b and JS8-6b; Fig. 2). Less than 12% of the NRM remained for the samples from sites JS8, JS9 and JS10 after heating up to 500 °C. AF demagnetization up to 120–140 mT left 3–12% of the NRM for sites JS1 to JS9 (e.g. samples JS1-3a, JS5-6a, JS7-3a; Fig. 2), whereas 65% of the initial magnetization remained for one sample from site JS10 (not shown). The exclusive normal polarity and the *in situ* direction parallel to the geocentric axial dipole magnetic field at the sampling areas support that this component is a recent (viscous or chemical) secondary magnetization (for stereographic projections of characteristic magnetic directions per sample from the La Laja and Zonda Formations, see Fig. 4A in Rapalini et al. (2000)). The La Flecha, La Silla and San Juan Formations (sites JS11 to JS23, in the Quebrada de La Flecha, Loma Redonda and Cerro Pedernal de los Berros areas) showed two components, a low unblocking temperature magnetization (<350 °C, for stereographic projections of mean site directions, see Fig. 4B in Rapalini et al. (2000)), coincident with Component A found in the La Laja and Zonda Formations (compare Zijderveld diagrams of samples JS1-3b, JS5-6b and JS7-3b with JS13-3b, JS15-2a, JS16-1a and JS22-3b), and a post-tectonic remagnetization of higher unblocking temperature (Component B) which was completely erased between 350 and 500 °C, suggesting that it is carried by (Ti-poor?) magnetite (e.g samples JS13-3b, JS14-2a, JS15-2a, JS16-1a, JS17-1a, JS22-3b, JS23-2a, JS20-5a, JS21-3b; Fig. 2). The AF demagnetization treatment defined clearly Component A, though it was less effective for identification of Component B (e.g. the latter can be observed in sample JS14-1a but not in sample JS13-3a; Fig. 2). The pole position corresponding to this last direction was associated with a late Permian post-folding remagnetization caused by the Sanrafaelic tectonic phase but previous to the Neogene uplift of the Eastern Precordillera. Rapalini et al. (2000) showed that Component B mean direction would match a Permian expected direction if untilting due to the Eastern Precordillera uplift is taken into account.

Hysteresis data from carbonates of the La Laja and Zonda Formations, not affected by the late Palaeozoic event, was shown to follow a SD + MD trend typical of non-remagnetized limestones (Dunlop, 2002a, b, Fig. 3) in a theoretical Day plot, while the remagnetized carbonates of the La Flecha, La Silla and San Juan Formations broadly fall within the SD + MD to SP + SD trends (Rapalini et al., 2000; Font et al., 2012). Remagnetized limestones from the Ponón Trehué Formation, in the San Rafael Block (Mendoza province), which were also affected by the Sanrafaelic overprint (Truco and Rapalini, 1996; Fazzito and Rapalini, 2016), are characterized by hysteresis parameters data that are restricted to the area between SD + MD and SP + SD mixing curves for magnetite and follow the trend of PSD + SP mixing curves. These samples show ratios of Mrs/Ms that are similar to those estimated for the remagnetized limestones of the San Juan Formation of the Eastern Precordillera.

## 4. Laboratory techniques, measurements and results

### 4.1. Magnetic mineralogy and rock-magnetic properties

Al least, one sample per site was subject to stepwise isothermal remanent magnetization (IRM) up to 2.3 T by means of an ASC Scientific IM-10-30 pulse magnetizer. Backfield demagnetization of IRM was subsequently imparted on some of them (16 samples). A low-coercivity magnetic phase, compatible with (titano?) magnetite, maghemite and/or pyrrhotite, is shown at each measured sample by a rapid acquisition, at low fields (<0.15 T), of isothermal remanent magnetization (Fig. 4). Slopes strongly change at ~0.1 T in several curves (e.g. JS6-5b, JS8-5, JS9-3b, JS11-5a, JS12-1b, JS23-5b and all samples from the San Juan Formation). At this point, 20–35% of the maximum IRM value is reached indicating that the soft-coercivity ferromagnetic phase is subordinate in volume with respect to the high-coercivity carriers. All the specimens, except for JS22-1b and perhaps JS23-5b, both from the La Silla Formation, are

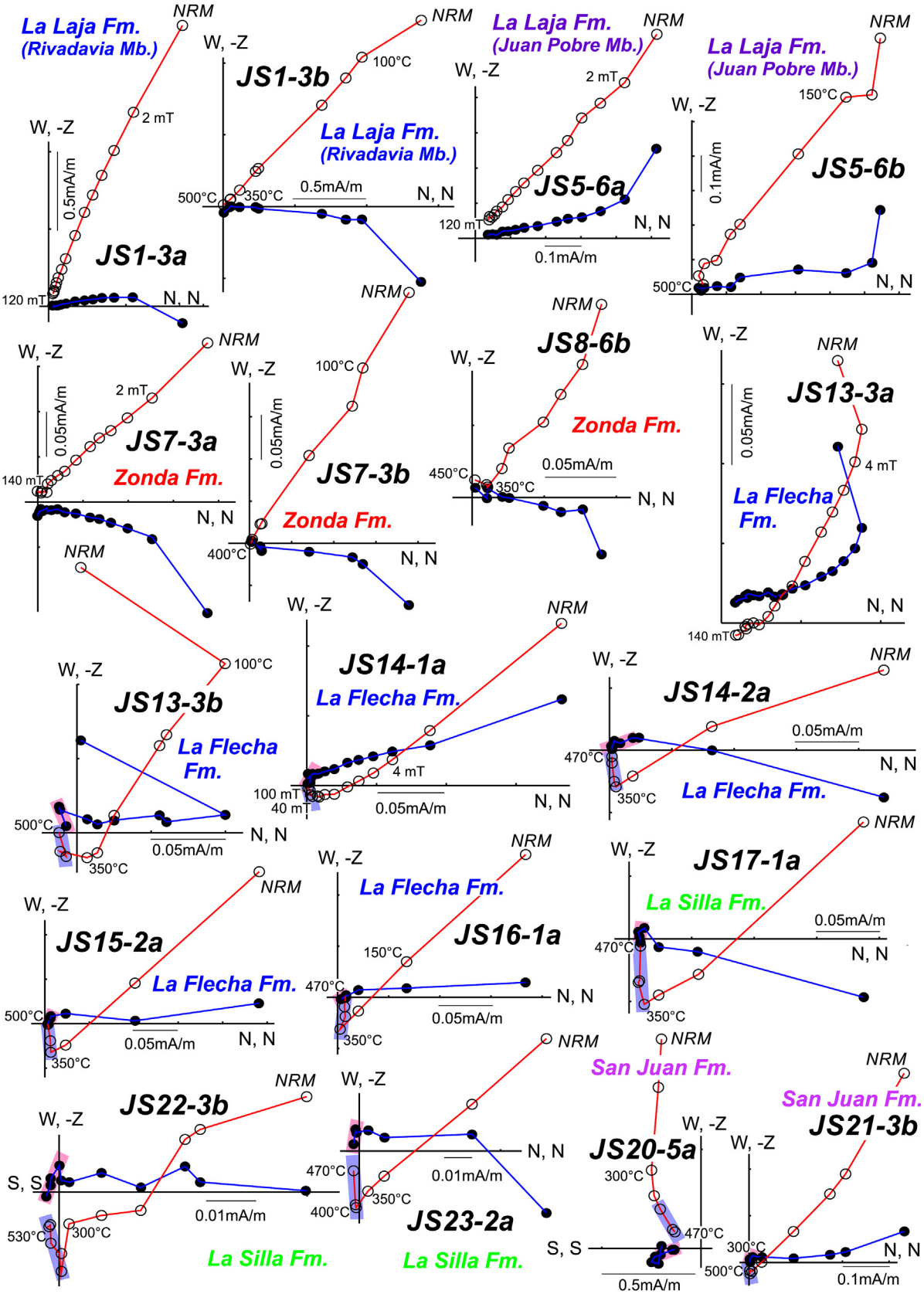


**Fig. 2.** Orthogonal vector plots (bedding corrected) of stepwise thermal or alternating field demagnetization of representative samples from the palaeomagnetic study carried out by Rapalini et al. (2000) in the La Laja, Zonda, La Flecha, La Silla and San Juan Formations. Open (solid) symbols point out vertical (horizontal) projection. Component B (vertical projection: thick violet line; horizontal projection: thick rose line) and meaningful demagnetization steps are shown. NRM: natural remanent magnetization. (For interpretation of the references to colour in this figure legend, the reader is referred to the web version of this article.)

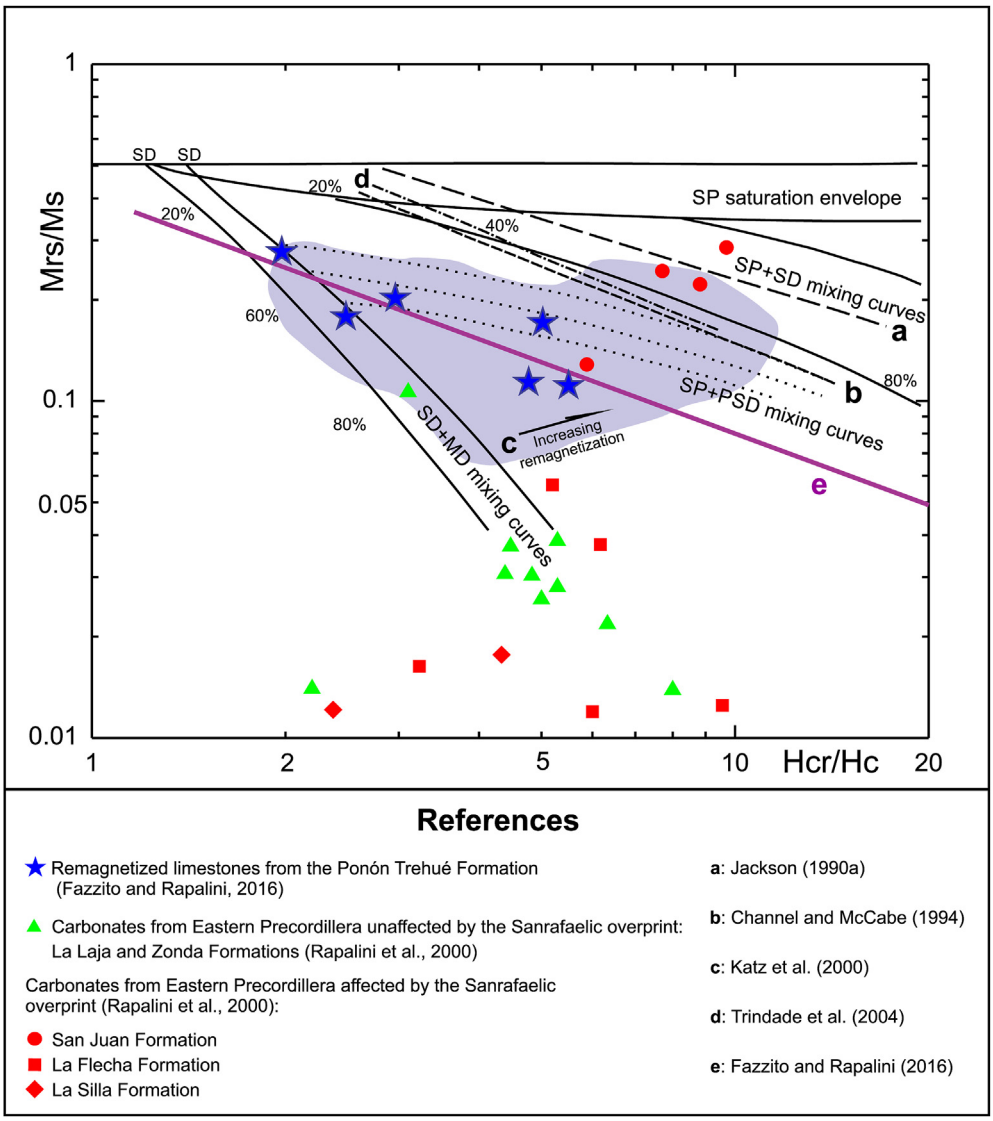


**Fig. 3.** Data for carbonates from Eastern Precordillera (Channell and McCabe, 1994; Rapalini et al., 2000) unaffected (green triangles) and affected (red squares, circles and diamonds) by the Sanrafaelic overprint and remagnetized limestones from the San Rafael Block (Ponón Trehué Formation, blue stars) compared to theoretical Day plot curves for magnetite (Dunlop, 2002a). Remagnetization field of limestones from Katz et al. (2000), as shaded area, and examples of worldwide fitted curves of remagnetized carbonates (modified from Font et al., 2012) are shown. (For interpretation of the references to colour in this figure legend, the reader is referred to the web version of this article.)

far from saturation at the maximum available field of 2.3 T, especially those from the La Laja and Zonda Formations, revealing that a high-coercivity (antiferromagnetic) phase, goethite and/or haematite, is a significant component of the ferromagnetic *s.l.* fraction. The unsaturated curves and the existence of a multi-modal distribution of coercivities for the entire collection of carbonates are clearly exhibited by plots with horizontal logarithmic scale (insets of Fig. 4). Backfield demagnetization curves (Fig. 4) indicate the presence of magnetic minerals with a wide range of values for the coercivity of remanence ($B_{cr}$). For the La Laja, Zonda, La Flecha and La Silla Formations, the magnitudes of $B_{cr}$ span from 47 mT to 485 mT, whereas for the San Juan Formation these values are restricted from 334 to 423 mT.

Stepwise thermal demagnetization of triaxial orthogonal IRM (Lowrie, 1990) at 2.0, 0.4 and 0.1 T along the *z*, *y* and *x* axes, respectively, was conducted in 17 representative specimens from the five formations. Thermal treatment at temperatures of 90 °C, 125 °C, 160 °C followed by steps of 50 °C, between 200 and 500 °C, and of 30 °C, between 530 and 650 °C, was subsequently applied using an ASC Scientific TD 48 SC furnace. Two samples from the La Laja Formation (one from the Rivadavia Member and one from the Juan Pobre Member), two samples from the Zonda Formation and one sample per site from the La Flecha, La Silla and San Juan Formations, were submitted to the Lowrie (1990) test (main results are shown in Fig. 5; additional 3D-IRM demagnetization plots can be found in Appendix 1). In the La Laja Formation (samples JS2-1 and JS6-2; Fig. 5a and b, respectively), the soft and the intermediate components indicate the unblocking of (Ti-poor?) magnetite at 450–500 °C; the hard component decays abruptly at around 90 °C revealing goethite and finally demagnetizes above 620 °C, also

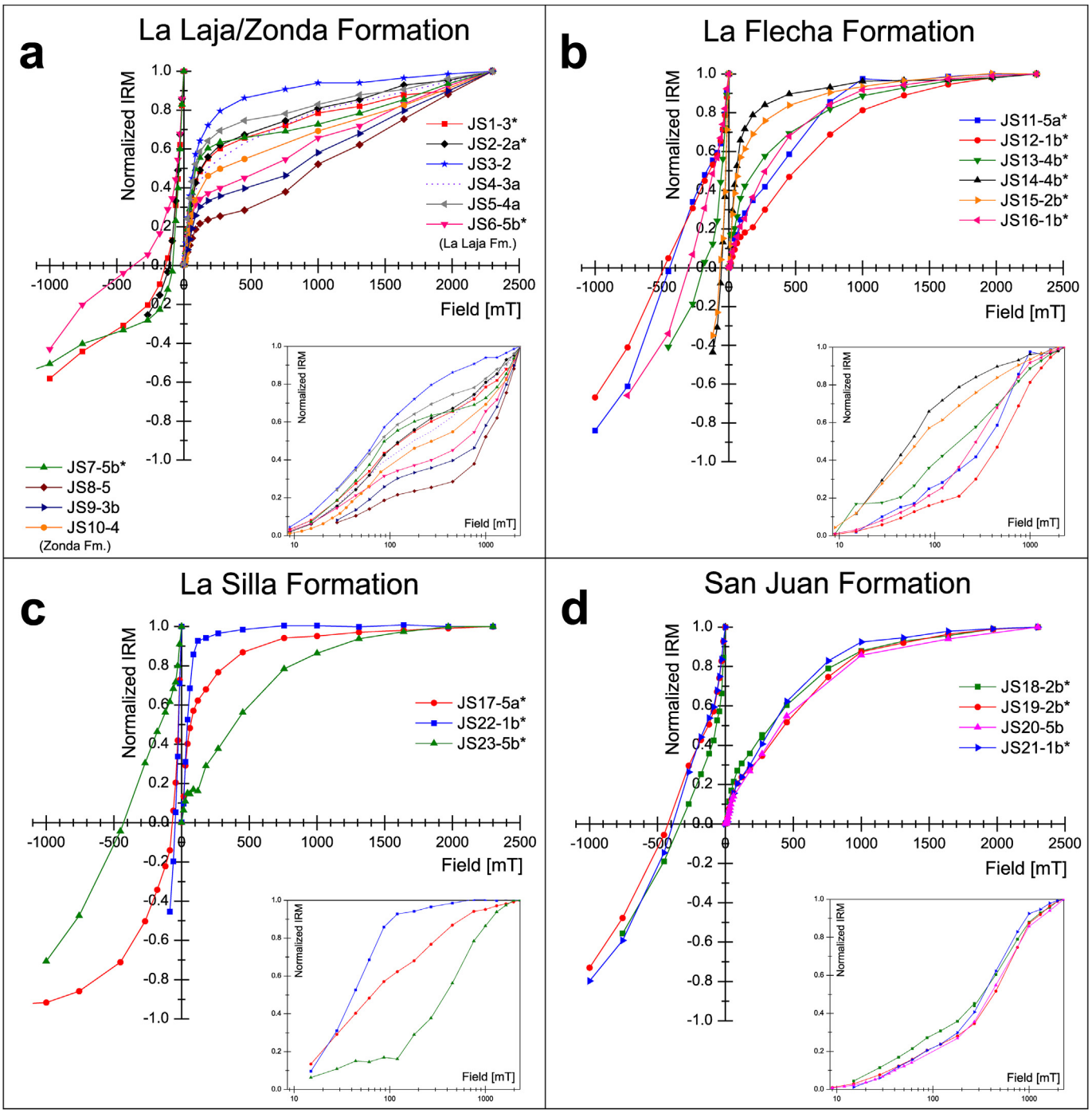


**Fig. 4.** Representative normalized isothermal remanent magnetization (IRM) curves acquired in magnetic fields up to 2.3 T and backfield demagnetization (only samples indicated by asterisk) from the five geologic formations: **a)** La Laja and Zonda, **b)** La Flecha, **c)** La Silla and **d)** San Juan. Insets: IRM curves with applied field in logarithmic scale.

showing the presence of some haematite. In the Zonda Formation (samples JS8-6 and JS10-1a; Fig. 5c and d, respectively), pyrrhotite is inferred by drops of the three components at ~300 °C, whereas (Ti-poor?) magnetite is shown by intensity decays between 450 and 500 °C in the soft and intermediate components, and goethite by a clear magnetization decrease at ~90 °C of the hard fraction; finally, some haematite is suggested by the total obliteration of magnetization at temperatures higher than 620 °C. In the La Flecha Formation, intensity drops at around 300 °C in the three components is suggestive of pyrrhotite (Fig. 5e, f, g and h), while decay of the soft and the medium fractions in the range 400–500 °C in several samples (Fig. 5f and g, Appendix 1a, 1b) indicate (Ti-poor?) magnetite content; the presence of haematite in some samples is suggested by deletion of the hard component at temperatures

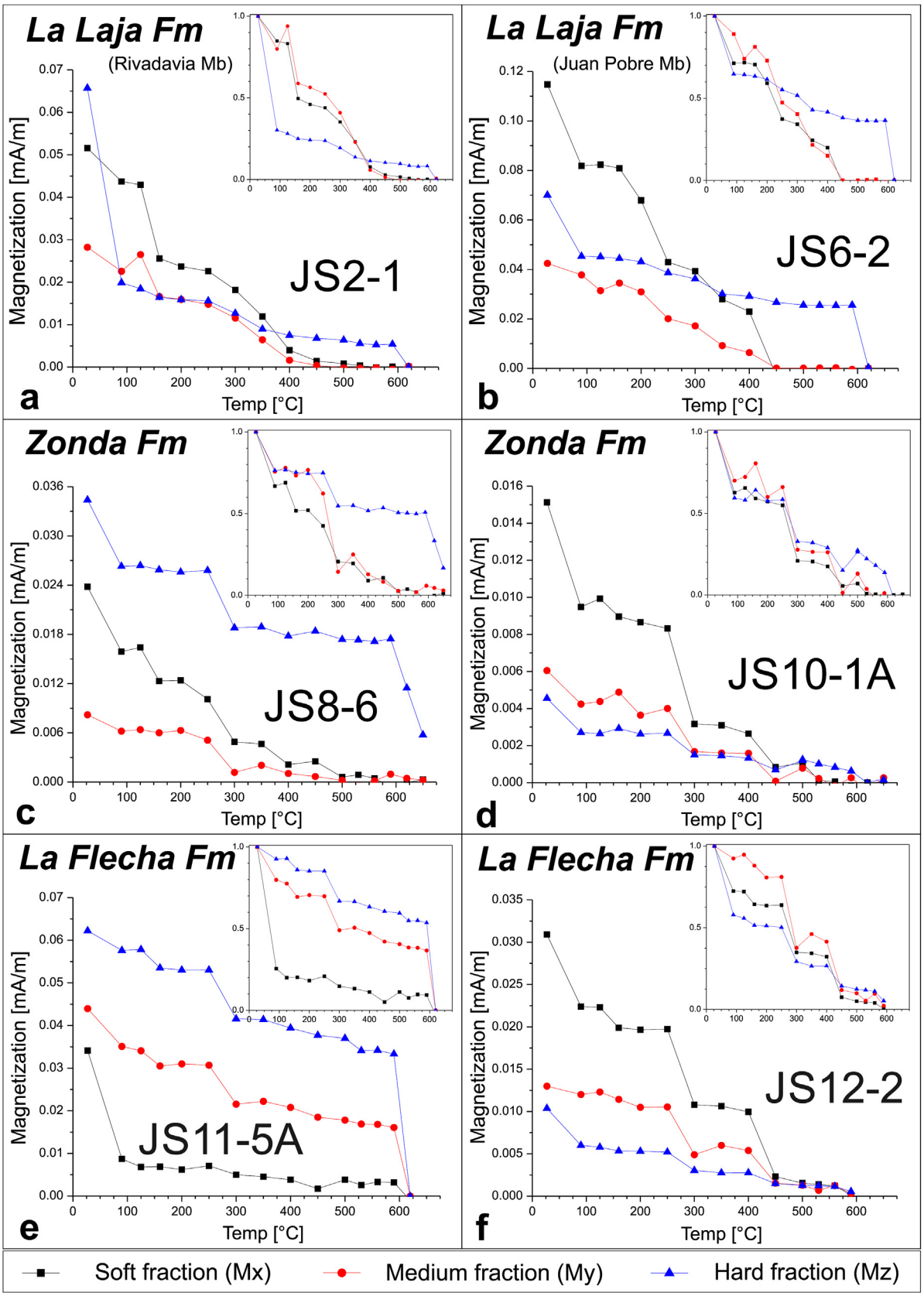


**Fig. 5.** Typical thermal demagnetization of three-component IRM (Lowrie, 1990) plots for specimens from the La Laja, Zonda, La Flecha, La Silla and San Juan Formations. Insets show curves normalized by the maximum intensity of the coercivity fraction.

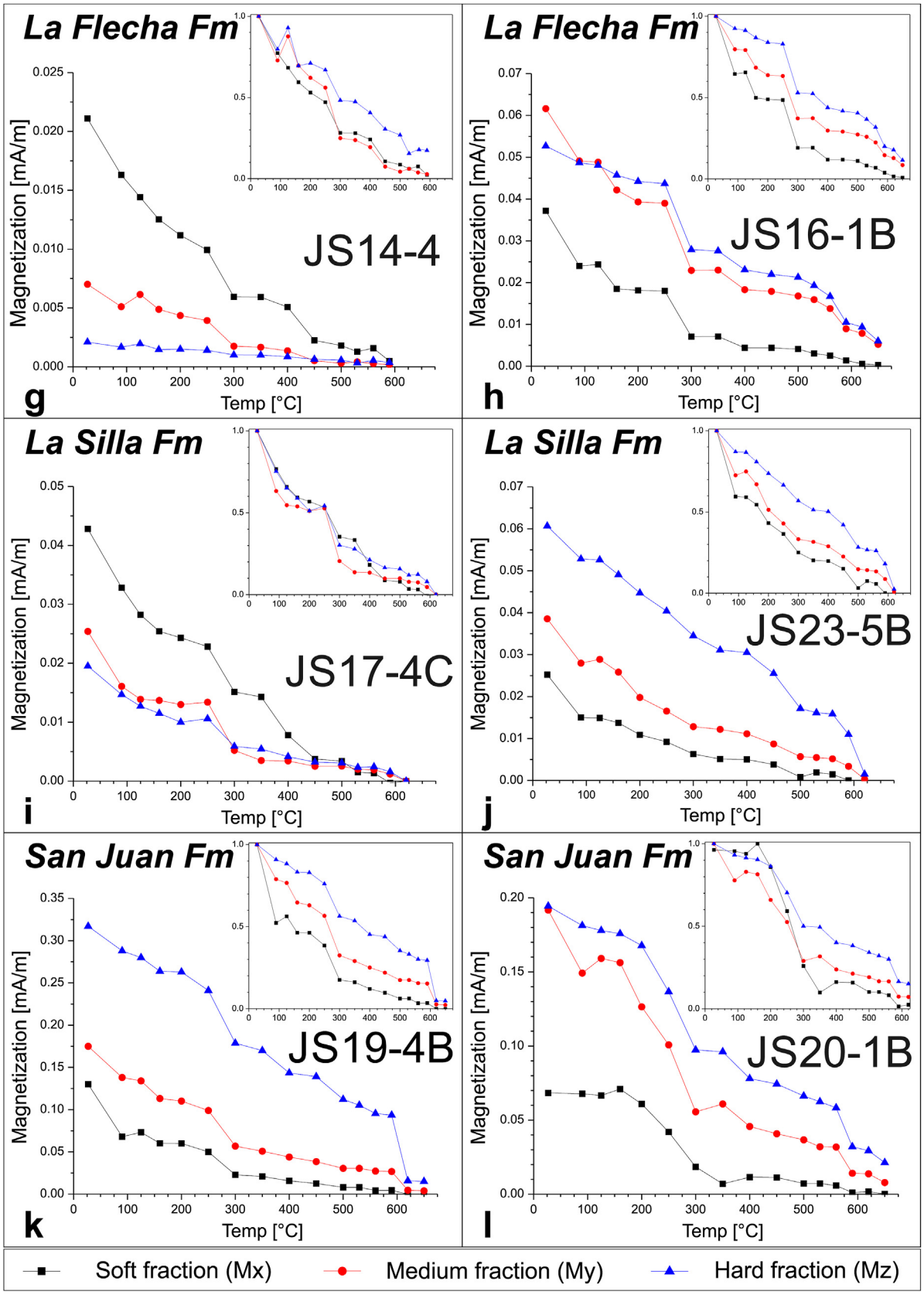


**Fig. 5.** (*continued*).

above 590 °C (Fig. 5e, f, h, Appendix 1b). In the La Silla Formation, the unblocking of pyrrhotite is only evidenced in sample JS17-4c (Fig. 5i) by a drop of intensity at 300 °C, in all fractions; the presence of (Ti-poor?) magnetite is suggested by the total demagnetization of the soft fraction in the range 400–590 °C in samples JS17-4c (Fig. 5i), JS22-1c (Appendix 1c) and JS23-5b (Fig. 5j) and also in the complete demagnetization of the medium fraction in sample JS22-1c at 450 °C; haematite content is supported by the complete demagnetization of the hard fraction in samples JS17-4c (Fig. 5i) and JS23-5b (Fig. 5j) at 620 °C. In the San Juan Formation, all components in samples JS18-2b (Appendix 1d), JS19-4b (Fig. 5k), JS20-1b (Fig. 5i) and JS21-1b (Appendix 1e) are partially unblocked in the range 300–350 °C, suggesting pyrrhotite; the total demagnetization of the soft fraction in the range 500–590 °C of samples JS18-2b (Appendix 1d), JS20-1b (Fig. 5i) and JS21-1b (Appendix 1e) indicates (Ti-poor?) magnetite, meanwhile the intensity of the medium and the hard coercivity axes of the four studied samples drops to zero at temperatures $\geq$ 620 °C revealing haematite content. A subordinate presence of goethite in samples from the La Flecha, La Silla and San Juan Formations may be subtly suggested by minor drops at 90 °C in the medium and/or hard fractions (e.g. JS11-5a, JS17-4c, JS20-1b). The soft fraction gives the highest contribution to the total IRM in one sample from the Zonda Formation (JS10-1a), four samples from the La Flecha Formation (JS12-2, JS13-5, JS14-4 and JS15-2b) and in two samples from the La Silla Formation (JS17-4c and JS22-1c). The hard fraction dominates the intensity of JS8-6 (Zonda Formation), JS11-5a (La Flecha Formation), JS23-5b (La Silla Formation) and all samples from the San Juan Formation (JS18-2b, JS19-4b, JS20-1b and JS21-1b). The contribution of the medium fraction to the total magnetization is similar to the soft fraction in samples JS2-1 and JS6-2 and to the hard fraction in sample JS16-1b. Maghemite was discarded as carrier of IRM because, in all samples except for JS14-4, the significant drops at 300–350 °C were observed not only in the medium fraction, but also in the hardest (typical values of coercivity of maghemite are lower than those of pyrrhotite, see Peters and Dekkers (2003)).

In general, for these carbonates, three axial IRM, which evaluates at the same time coercivities and unblocking temperatures of magnetic minerals, resulted a robust method compared to a coercivity component analysis over IRM data (Kruiver et al., 2001). While in some samples the Lowrie (1990) test was able to discriminate up to four carriers of isothermal remanence, bimodal distributions were typically observed in the gradient acquisition plots (GAP); this is probably due to overlapping coercivities spectra of the pairs pyrrhotite/(Ti) magnetite and haematite/goethite. Therefore, quantitative analyses of IRM acquisition curves was considered of little value to elucidate the magnetic mineralogy of our study samples.

Temperature dependence of low-field magnetic susceptibility (976 Hz, 200 $Am^{-1}$) from room temperature to ~660 °C was studied by using an AGICO Kappabridge KLY-3S coupled to a CS-3 furnace in representative samples of the studied formations. An argon-controlled atmosphere to prevent oxidation was sustained while heating. Ferromagnetic mineralogy inferred from high-temperature thermomagnetic curves (representative curves are shown in Fig. 6) supports the results of the previous measurements. Irreversible cooling curves, with susceptibility rapidly increasing at temperatures below 580 °C, suggest creation of magnetite during thermal treatment. A minor decay of magnetic susceptibility in samples JS3-5a (La Laja Formation), JS10-2a (Zonda Formation), JS16-4 (La Flecha Formation) and JS20-3a (San Juan Formation), from room temperature up to about 100 °C, is consistent with the presence of some goethite (Fig. 6). Pyrrhotite content is suggested by the drop of susceptibility values in the range 265–310 °C in sample JS16-4 (Fig. 6c) and by the susceptibility decrease between 280 and 350 °C in sample JS20-3a. A soft decrease of susceptibility between 250 and 300 °C in sample JS3-5a (Fig. 6a) may also be indicating some pyrrhotite. All curves increase sharply at ~400 °C and then decrease abruptly at ~580 °C, indicating magnetite, but due to the irreversible character of the curves, discriminating between original magnetite from that produced due to heating is not possible. No clear evidence of haematite is observed for any sample in addition to a minor decreasing tail between 580° and 600 °C in most of the curves. However, as already mentioned, significant formation of magnetite during heating above 400 °C turns any interpretation of the curves above that temperature elusive and highly speculative.

Variation of bulk magnetic susceptibility with field amplitude between 2 and 700 $Am^{-1}$ (976 Hz) was studied in 8 samples representative of the five geologic formations with an AGICO Multifunction Kappabridge (MFK1-FA). The analysis of variation of magnetic susceptibility *vs* field amplitude is considered only for values above 5 $Am^{-1}$ since measurement noise is important below this intensity for all samples (curves normalized by the minimum value of magnetic susceptibility are shown in Fig. 7). A minor scatter of magnetic susceptibility is still observed for fields in the range 5–100 $Am^{-1}$ for most samples. Two samples, JS7-1 (Zonda Formation) and JS17-6 (La Silla Formation) showed the greatest dispersion below 100 $Am^{-1}$. In the range 5–700 $Am^{-1}$, the total variation of magnetic susceptibility is usually below 11%. The curves show a decrease in bulk susceptibility with increasing field in the entire range, with the only exception of sample JS17-6 in the interval 100-300 $Am^{-1}$, which presents a small linear increase. This fall is slight for fields up to 100 $Am^{-1}$ and more abrupt for fields higher than 250-350 $Am^{-1}$. This type of decreasing curves in a wide field range has been reported previously in some fine-grained keratophyre, loess, sedimentary rocks and rocks with single domain magnetite (Hrouda et al., 2006a), though an explanation for the origin of its nature has not been suggested yet. The fact that these carbonates showed non-increasing curves suggests that the influence of pyrrhotite in magnetic susceptibility is likely subordinate to negligible since this mineral is characterized by notorious increasing curves (Hrouda et al., 2006a, b). Titanomagnetite also produces increasing susceptibility curves, with slopes directly related with the amount of titanium, therefore pure magnetite or titanomagnetite with very low Ti content is also suggested. These results are broadly consistent with other rock-magnetic data, already reported, like the fact that most of the NRM was almost completely erased below 500 °C and that the soft component in thermal demagnetization of 3D-IRM was unblocked at ~500 °C.

Magnetization hysteresis loops were obtained from −1 to 1 T in one sample per site by using a Molspin Vibrating Sample Magnetometer. Diamagnetic and paramagnetic effects were corrected by subtracting the high-field slope. Magnetic hysteresis loops show, at high fields, a predominant paramagnetic (e.g. inset of Fig. 8a), diamagnetic (e.g. insets of Fig. 8b and e) or ferromagnetic influence (insets of Fig. 8c, d and f). Actually, all samples from the La Laja Formation show a dominant paramagnetic contribution, while those from the Zonda Formation show either dominant diamagnetic or ferromagnetic patterns (Appendix 2). With the exception of a couple of samples from the La Silla Formation, all other analysed samples from the La Flecha, La Silla and San Juan Formations (units that carry the Sanrafaelic remagnetization) present hysteresis loops of dominant ferromagnetic character (see Appendix 2). This

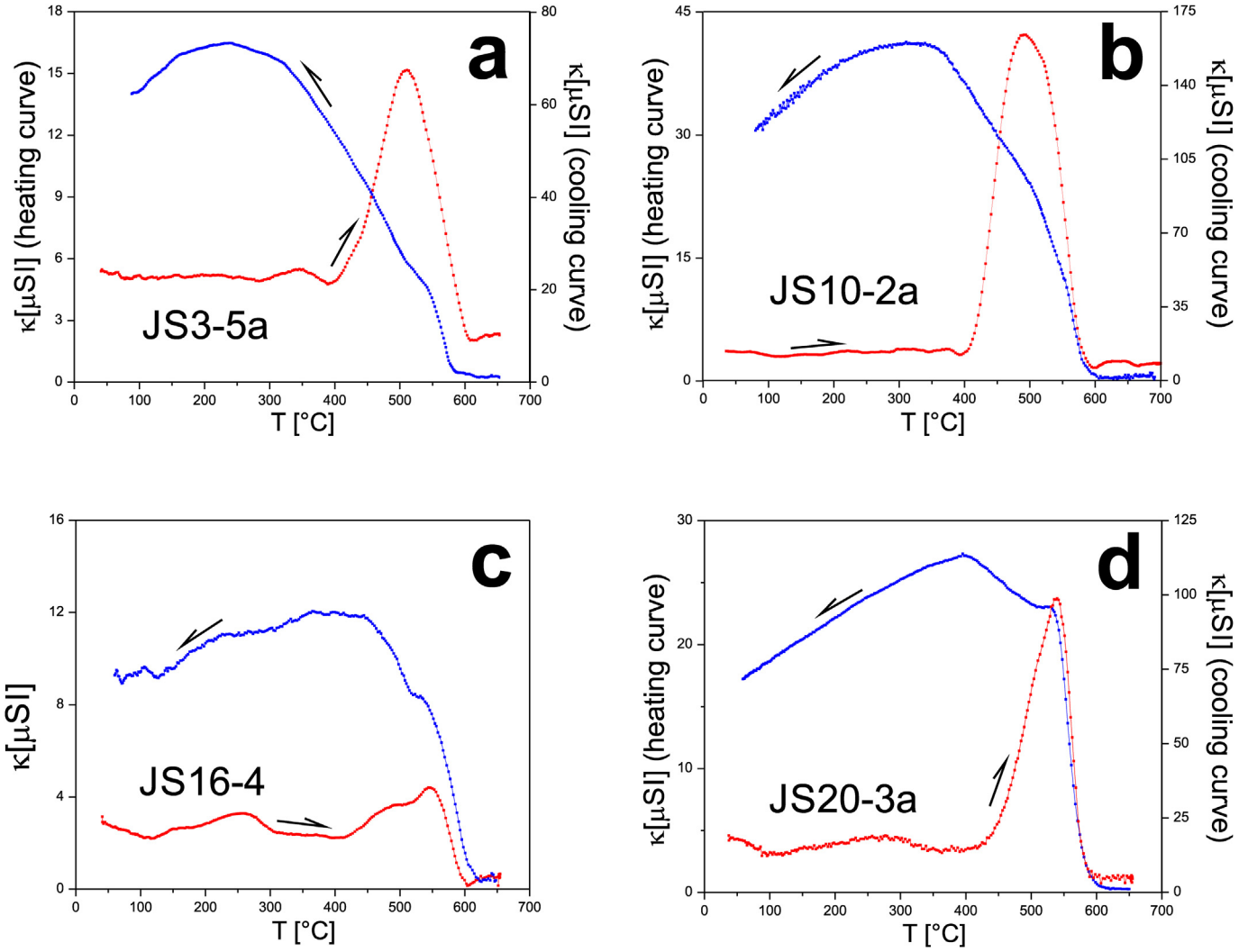


**Fig. 6.** Characteristic high-temperature thermomagnetic curves of samples from the carbonate sequence. Heating (red) or cooling (blue) sense is indicated by arrows. (For interpretation of the references to colour in this figure legend, the reader is referred to the web version of this article.)

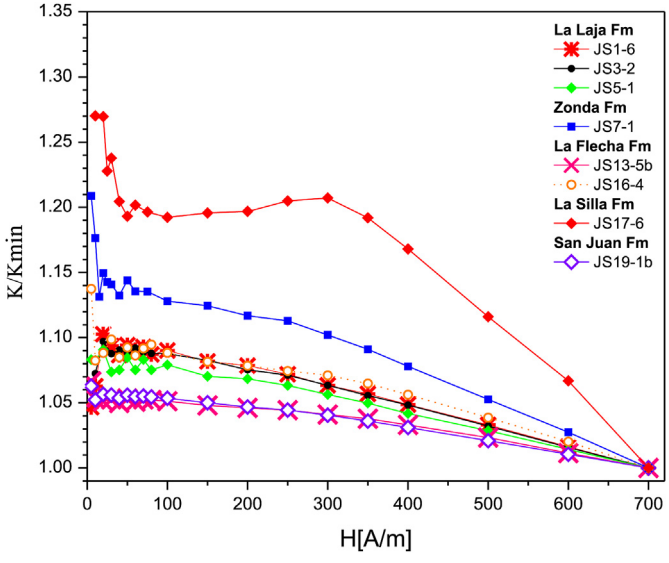


**Fig. 7.** Field dependence of bulk magnetic susceptibility up to 700 $Am^{-1}$ (976 Hz) in samples from the five geologic units.

observation suggests a correlation of the character of the hysteresis loops with the presence or absence of the Sanrafaelic remagnetization. Smoothing of the noisy curves was applied to improve the definition of their shape after subtraction of the high-field diamagnetic or paramagnetic slope (Fig. 8 and Appendix 2). All hysteresis loops from the five formations, except for sample JS10-2a (see Appendix 2), are slightly to strongly wasp-waisted. The La Laja and the Zonda Formations (Fig. 8a and b) and one sample from the San Juan Formation (JS21-3a, Appendix 2) present very slim loops. Broader hysteresis loops are determined for the rest of the sites (Fig. 8c–f). The widest hysteresis loops are found in two samples from the La Flecha Formation (JS11-2a and JS 12-4a; Fig. 8c and Appendix 2, respectively) and in most from the San Juan Formation (JS18-3a, JS19-7a and JS20-3a; Fig. 8f and Appendix 2). The constriction of the loops is probably related to the presence of different magnetic minerals with contrasting coercivities indicating a mixture of a hard (antiferromagnetic) and a soft (ferromagnetic) mineral. However, the presence of a relatively large proportion of superparamagnetic (SP) grains may also contribute to it, as described below. Constricted hysteresis loops are considered a worldwide signature of remagnetized carbonates (Kodama, 2012).

The evaluation of thermal demagnetization diagrams of NRM (Rapalini et al., 2000), acquisition and backfield curves of IRM,

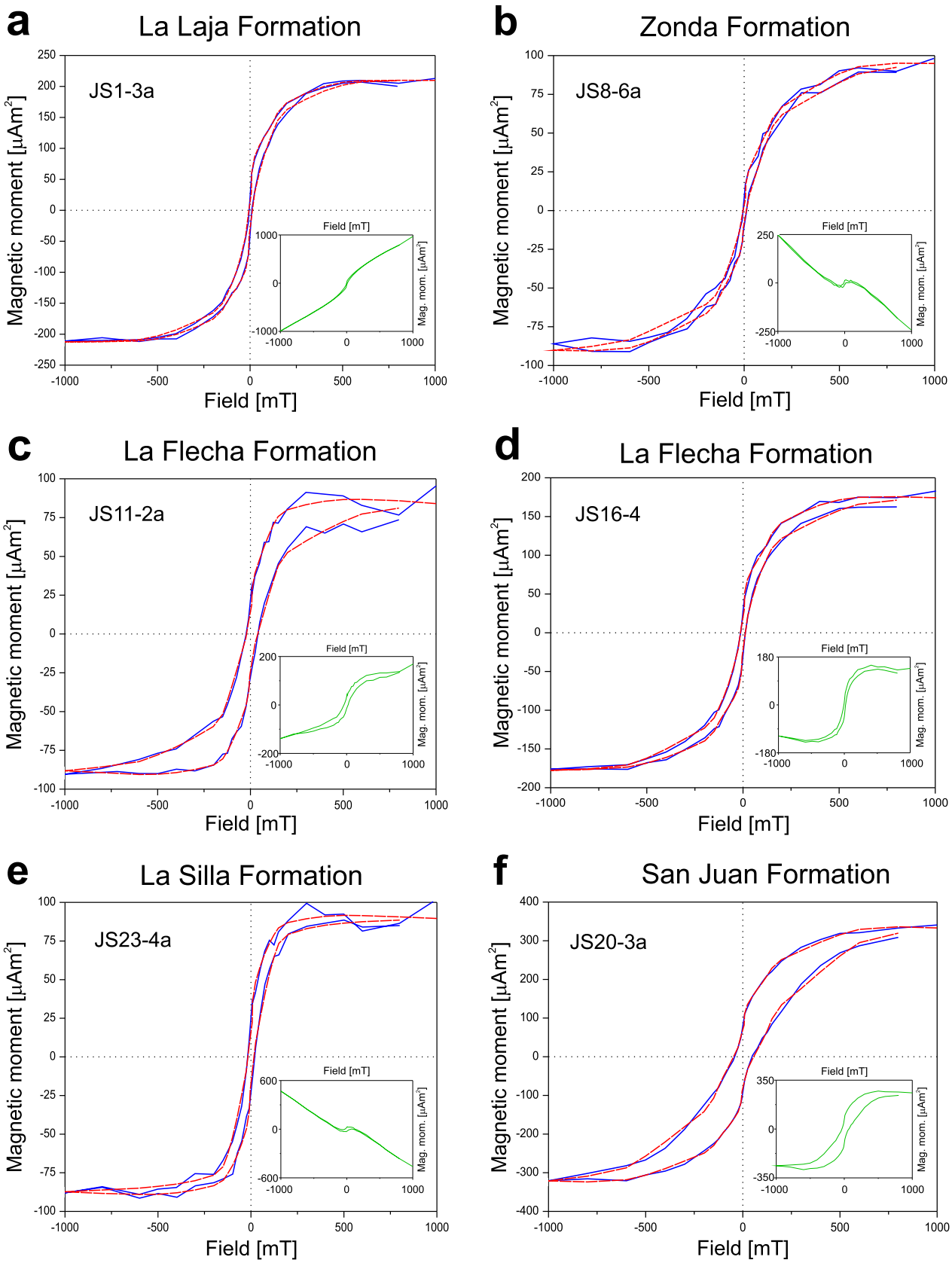


**Fig. 8.** Hysteresis loops from the five carbonate units after subtraction of diamagnetic or paramagnetic high-field slope (blue). Red dashed line: smoothed curve. Insets: raw data before correction (green). (For interpretation of the references to colour in this figure legend, the reader is referred to the web version of this article.)

thermal demagnetization of three-axis IRM, thermomagnetic curves and hysteresis loops, reveal consistent information about the complex mineralogy of these carbonates and about the carriers of remanence. In sites JS1 to JS10 the single remanence (Component A, La Laja and Zonda Formations), with unblocking temperatures below 500 °C, is carried by (titano?) magnetite. Thermal demagnetization of NRM and of three-axis IRM suggest that, in some samples of the Zonda Formation (e.g. sample JS8-6b, Fig. 2), this component may be carried also by pyrrhotite. Haematite is a very subordinate carrier of remanence in sites of the La Laja and Zonda Formations, although its presence explains the minor residual magnetization at temperatures >500 °C for some samples. Goethite/haematite content is consistent with the small residual remanence after the 120-mT or 140-mT AF demagnetization step (e.g samples JS1-3a, JS5-6a and JS7-3a, Fig. 2) and the $B_{cr}$ values above 100 mT inferred from backfield curves (Fig. 4a). The hard fraction dominates demagnetization of a triaxial IRM in one out of four studied samples from the La Laja and Zonda Formations (see sample JS8-6, Fig. 5c). The subordinate influence of the high coercivity phase for these sites is also evidenced in the small decays of magnetic susceptibility at ~100 °C (Fig. 6), in minor tails in thermomagnetic curves above 580 °C (Fig. 6) and in slim hysteresis loops (Fig. 8a and b). In sites JS11 to JS23 (La Flecha, La Silla and San Juan Formations), unblocking temperatures up to 350 °C shown by thermal demagnetization of NRM (Fig. 2) and of composite IRM (Fig. 5), indicate that Component A probably resides in pyrrhotite. (Titano?) magnetite carries Component B, considering its unblocking temperatures are around 500 °C. Magnetic properties on samples from the lower part of the La Flecha Formation, the upper part of the La Silla Formation and from the San Juan Formations normally indicated the presence of a high coercivity mineral (haematite). Backfield curves for some sites of these units (JS11, JS12, JS18, JS19, JS20, JS21 and JS23, Fig. 4b, c and e) showed high values of $B_{cr}$ (~500 mT). Medium and hard fractions dominate the demagnetization of triaxial IRM (sites JS11, JS18, JS19, JS20, JS21 and JS23, e.g. Fig. 5e and j-l). The widest hysteresis loops were obtained in sites JS11, JS12, JS18, JS19, JS20 and JS23 (e.g. Fig. 8c, e and f). However, haematite seems to contribute in a subordinate way to the NRM. On the other hand, most sites from the medium part of the section (La Flecha and La Silla Formations) are characterized by dominance of the soft coercivity fraction (magnetite). For sites JS13, JS14, JS15, JS17 and JS22 the highest contribution to the 3D- IRM is given by the soft component (e.g. Fig. 5g and i). The $B_{cr}$ values for sites JS14, JS15, JS17 and JS22 are below 100 mT, as determined from backfield curves (Fig. 4 b and c). This is consistent with hysteresis loops of intermediate width at the intermediate stratigraphic levels.

Interaction degree, effective grain size and domain state (Symons and Cioppa, 2000) were evaluated by performing the Cisowski (1981) test in one sample per geologic unit. The modified Lowrie-Fuller test (Johnson et al., 1975) was applied later as diagnostic for remagnetization in carbonates. For these analyses, the anhysteretic remanent magnetization (ARM) was acquired in a maximum alternating field of 100 mT with a steady field of 50 μT. Stepwise AF demagnetization of ARM and IRM was applied up to 100 mT (3-mT steps from 3 to 15 mT, 5-mT steps from 15 to 40 mT, 10-mT steps from 40 to 60 mT and 20-mT steps from 60 to 100 mT). The anhysteretic remanence was generated by using an AGICO AMU-1 magnetizer. AF demagnetization treatment was applied with an AGICO LDA-3A tumbler demagnetizer. Magnetic remanence was measured in every case by means of an AGICO JR-6 spinner magnetometer. A requirement for accurately applying the Cisowski (1981) test is reaching saturation of IRM. Considering that in these samples the Sanrafaelic remagnetization is carried by a low-coercivity phase (magnetite), the IRM was acquired up to 180 mT in order that the contribution to the IRM from the higher coercivity phases (pyrrhotite, haematite and goethite) is minor or negligible. The intersection point R between the IRM acquisition and AF demagnetization of IRM as a function of the applied field (Fig. 9), determines *x* values ranging from 39 to 69 mT and *y* values bracketed between 0.36 and 0.55. The values of the abscissa corresponding to the intersection points are an approximation of the coercive force, $B_{cr}$ (Cisowski, 1981). The curves of acquisition and demagnetization of IRM are in general quite symmetrical up to ~ $B_{cr}$, indicating non-interacting SD particles. For higher values the curves lose symmetry, probably as an effect of the presence of minerals of higher coercivity. The modified Lowrie-Fuller test (Johnson et al., 1975) indicates for all the samples that the ARM is less stable to demagnetization than the IRM, suggesting a dominance of a coarse-grained fraction. These constrasting results have been observed in magnetite-bearing remagnetized carbonates (Lowrie and Heller, 1982; Jackson, 1990a), in samples containing pyrrhotite and haematite (Trindade et al., 2004; Font et al., 2006), and it is characteristic of the Middle Ordovician Ponón Trehué limestones that carry the Sanrafaelic remagnetization (Fazzito and Rapalini, 2016).

### 4.2. Magnetic susceptibility, anhysteretic susceptibility and magnetic fabrics

In order to shed light on the origin of the Sanrafaelic remagnetization in the Eastern Precordillera, a systematic magnetic fabric study was carried out along the whole succession of carbonates.

Chemical composition data throughout the study succession (after Bordonaro, 2002) are plotted together with the variation of representative magnetic properties as a function of the stratigraphic height for the La Laja, Zonda, La Flecha, La Silla and San Juan Formations (Fig. 10).

The industrial exploitation of the five studied formations is of great economic relevance for the region since they are source for aerial, hydraulic, high-calcium and dolomitic lime, natural and Portland cement, iron and steel for smelting, calcium carbide, etc (Bordonaro, 1983, 2002; Arroqui Langer et al., 2006). Chemical analyses over more than a thousand samples all over the sequence (Fig. 10b and c) were reported by Bordonaro (2002). The sampled Rivadavia Member of the La Laja Formation carries 80–90% of calcium carbonate ($CaCO_3$) and less than 5% of magnesium carbonate ($MgCO_3$). Free silica ($SiO_2$) is absent. The Juan Pobre Member of the La Laja Formation, on the other hand, presents a variation of $CaCO_3$ between ~40 and 90% and abundant insoluble residues, iron oxides, alumina and silicates. The $MgCO_3$ ratio can be as much as 40% in the upper part of this member. The lower member of the Zonda Formation possesses 40–44% of $MgCO_3$, no more than 2% of insoluble residue and a very low content of Fe, P and S. Limestone, dolostone and chert intercalate regularly in the La Flecha Formation. Dolomitic levels ($\leq$25 m) reach up to 40% of $MgCO_3$ with insoluble residue $\leq$ 3%. These are commonly contaminated with chert. $CaCO_3$ rate can be as much as ~80% in the upper part of the unit. The La Silla Formation presents the highest rate of $CaCO_3$ of the entire sequence, with values up to 99%. The insoluble residue is less than 1%, the S and P content 0.03% and 0.01%, respectively. It has no free silica. The San Juan Formation contains 60–80% of $CaCO_3$, less than 10% of $MgCO_3$ (Bordonaro, 1983), more than 10% of insoluble residue and a high content of Si, Al and Fe. The

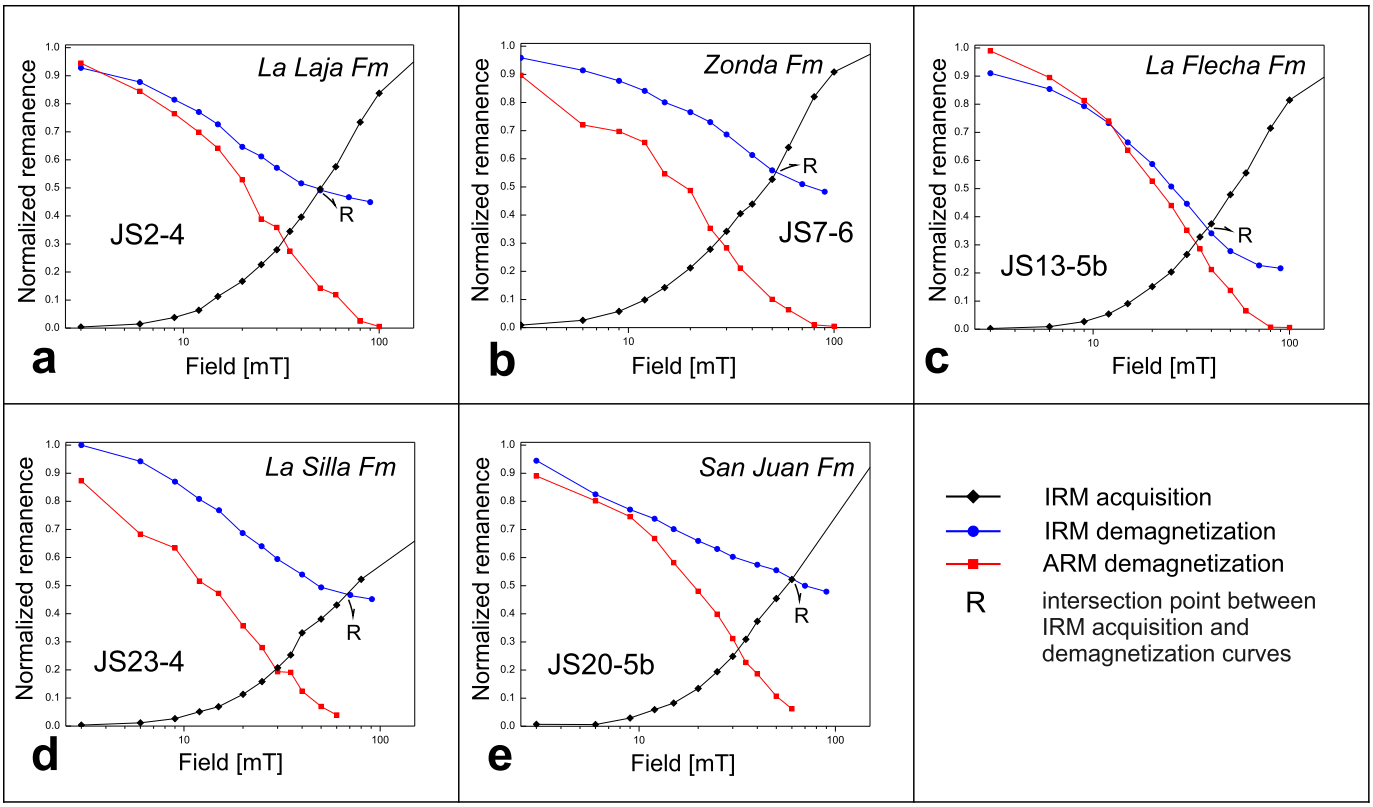


**Fig. 9.** Curves for the modified Lowrie-Fuller (Johnson et al., 1975) and Cisowski (1981) test for each sampled formation.

intercalation of chert is frequent.

Mean NRM intensities, available from measurements by Rapalini et al. (2000), were calculated over two up to eight specimens per site (Fig. 10d). Values of IRM at 0.12, 0.27 and 1.97 T (Fig. 10e) were in general obtained from one sample per site but, when possible, up to three values of IRM per site were averaged. Mean magnetic (Fig. 10f) and anhysteretic (Fig. 10g) susceptibilities were obtained from AMS and AARM measurements, respectively.

Bulk magnetic susceptibility was measured, ten times per sample, at two different frequencies, $f_1$ (976 Hz) and $f_3$ (15,616 Hz), at a field amplitude of 200 $Am^{-1}$, on several specimens per unit by employing a MFK1-FA susceptibility-metre. Considering mean values, the frequency dependence parameter $k_{fd}$ (%) = 100 × ($k_{f1}$-$k_{f3}$)/$k_{f1}$ (Dearing et al., 1996) was determined for each of these samples after correction for diamagnetic contribution. Weak bulk magnetic susceptibility values characterize the samples from the five units in Eastern Precordillera ($-1.17 \times 10^{-5} \leq \kappa \leq 1.20 \times 10^{-4}$ SI), either at low or at high frequency. The frequency-dependence parameter $k_{fd}$ in the carbonate rocks was calculated after applying a compensation for diamagnetic susceptibility which was taken as the intrinsic susceptibility of pure calcite at room temperature ($-12.09 \pm 0.50$) × $10^{-6}$ SI determined by Schmidt et al. (2006). The parameter $\kappa_{fd}$ ranges between 2 and 17% (Fig. 10h), but for most samples this value is above 5%, as it is usually found in remagnetized carbonates (Jackson et al., 1993; Font et al., 2006, 2011a, b). In particular, $\kappa_{fd}$ is greater than 5% in all samples from the La Laja and San Juan Formations. A medium to high concentration of superparamagnetic (SP) grains is associated with these percentages (Dearing et al., 1996). The presence of significant quantities of SP grains can explain natural remanent magnetization carried by pure magnetite with relatively low unblocking temperatures (<500 °C), as observed in the original palaeomagnetic study by Rapalini et al. (2000), with no need to invoke Ti-poor titanomagnetite for them (see for example Zegers et al., 2003). SP grains are also an alternative source for the wasp-waisted character of most hysteresis loops of these carbonates.

The anisotropy of low-field AC (200 $Am^{-1}$, 976 Hz) magnetic susceptibility was determined in 20 sites (172 specimens) with the MFK1-FA Kappabridge in the 15-position protocol. Mean anisotropy factors (Tarling and Hrouda, 1993) per site such as $P_J$ (corrected anisotropy degree), $L$ (magnetic lineation) and $F$ (magnetic foliation) were estimated. The mean magnetic susceptibility $k_m$ is very low for all sites ($-1.10 \times 10^{-5} \leq \kappa_m \leq 8.61 \times 10^{-5}$ SI, Fig. 10f, Table 2). The lowest mean magnetic susceptibilities ($\kappa_m \leq 3.29 \times 10^{-5}$SI) were determined at the Zonda, La Flecha and La Silla Formations, whereas the highest mean magnetic susceptibilities ($\kappa_m \geq 3.83 \times 10^{-5}$ SI) were measured at the La Laja and San Juan Formations. A broad correlation is observed between several magnetic parameters and the dolomitic content (Fig. 10). Highest $MgCO_3$ coincides with lowest values of NRM intensity and of the IRM intensity (particularly of the soft and medium fraction), low mean magnetic susceptibility, anhysteretic susceptibility and frequency-dependent parameter. This suggests a strong influence of dolomitization processes in the value of the magnetic parameters, mainly associated with amount of ferromagnetic fraction. This also is suggested by the fact that all specimens from sites JS9 (Zonda Formation), JS10 (Zonda Formation), JS11 (La Flecha Formation), JS12 (La Flecha Formation), JS22 (La Silla Formation) and JS23 (La

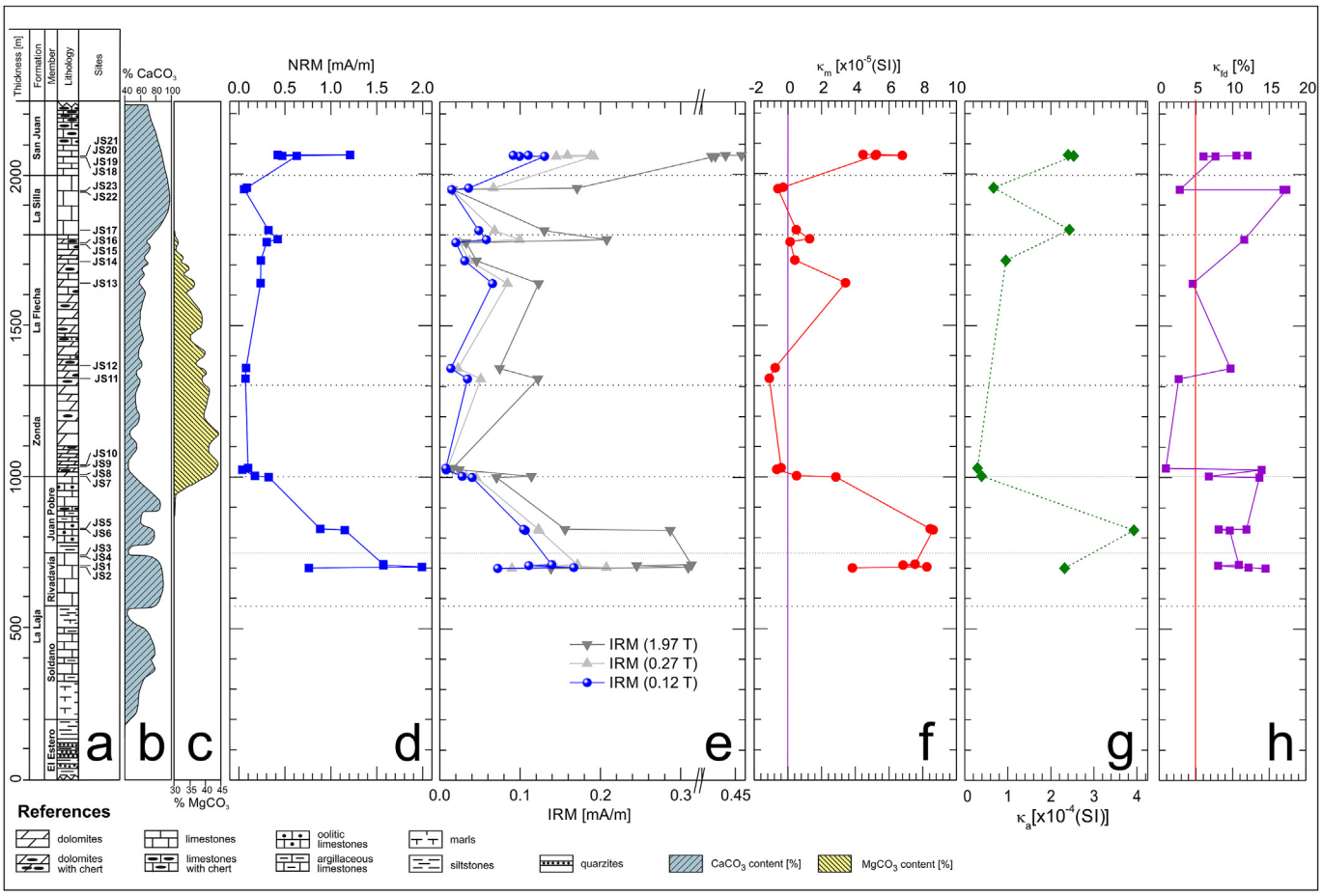


**Fig. 10.** **a)** Stratigraphic distribution of palaeomagnetic sampling sites. Modified from Baldis and Bordonaro (1984) and Rapalini et al. (2000). **b)** Calcite and **c)** dolomite content in percentage (Bordonaro, 2002). Site-mean magnitudes of: **d)** natural remanent magnetization, **e)** isothermal remanent magnetization at 0.12, 0.27 and 1.97 T, **f)** magnetic susceptibility $\kappa_m$ and **g)** anhysteretic susceptibility $\kappa_a$, as a function of the stratigraphic height. **h)** Variation of frequency dependence parameter $\kappa_{fd}$ (corrected by diamagnetic contribution to the magnetic susceptibility) for selected samples of the five studied formations. The value of 5% has been highlighted.

Silla Formation) are diamagnetic, as well as two of five specimens from site JS15 (La Flecha Formation). The Zonda and La Flecha Formations show the highest content of magnesium carbonate (Fig. 10).

Though several examples of AMS and AARM studies in remagnetized carbonates can be found in the literature (e.g. McCabe et al., 1985; Jackson et al., 1989; Ihmlé et al., 1989; Jackson, 1990b; Rochette et al., 1992; Lu and McCabe, 1993; Evans et al., 2003; Fazzito and Rapalini, 2016), systematic research is still scarce. A southern extension of the carbonate platform of the Argentine Precordillera is exposed in the San Rafael Block (Mendoza province, central-western Argentina) as the Middle Ordovician limestones of the Ponón Trehué Formation. These carry a syntectonic Permian remagnetization associated with the Sanrafaelic event (Truco and Rapalini, 1996). A recent magnetic fabric study (Fazzito and Rapalini, 2016) on these rocks suggested a secondary origin for the magnetic fabric and that the carriers of the remagnetization (magnetite plus pyrrhotite) were chemically precipitated in the local stress regime at the last stages of folding. A systematic magnetic fabric study was, therefore, performed in all sites of Eastern Precordillera. Unfortunately, only two remaining samples per site were available from the original study (Rapalini et al., 2000) at sites JS11 (La Flecha Formation), JS18 and JS21 (San Juan Formation). Although mean magnetic susceptibility is calculated for these sites, anisotropy parameters and statistical directional analysis are not available. For the remaining sites, susceptibility ellipsoids are in general well-defined (Figs. 11 and 12). The anisotropy of magnetic susceptibility for diamagnetic specimens was analysed in terms of the convention of Borradaile et al. (2012). The direction of the most negative susceptibility corresponds to the minimum axis ($K_3$) while the direction of the least negative axis is defined as the maximum axis ($K_1$). This rule produces paramagnetic-compatible fabrics.

Eight out of ten sites from the La Laja and the Zonda Formations (Figs. 11 and 12) are characterized by an inverse relation of the magnetic susceptibility fabric with respect to the structural features (i.e. $K_1$ is orthogonal to the bedding plane), while two sites, JS5 and JS7, show an intermediate fabric ($K_3$ is contained in the bedding plane). Two inverse (JS12 and JS16) and three intermediate (JS13, JS14 and JS15) magnetic fabrics were identified in the La Flecha Formation. The La Silla Formation presents one site with inverse magnetic fabric (JS17), one with intermediate (JS22) and one with normal (JS23, $K_3$ orthogonal to the bedding plane) magnetic fabric. The San Juan Formation exhibits a normal magnetic fabric at site JS19, while the following site (JS20) shows an

**Table 2**
Mean anisotropy parameters for magnetic susceptibility (ASM) and anhysteretic remanence (AARM) fabrics for the La Laja (LL), Zonda (Z), La Flecha (LF), La Silla (LS) and San Juan (SJ) Formations. Fm: geologic formation; Lat/Long: latitude and longitude of the sampling location; SC: structural correction; Dec: declination; Inc: inclination; n, number of measured specimens per site; $\kappa_m$, magnetic susceptibility (in $10^{-6}$, SI); $\kappa_a$, anhysteretic susceptibility (in $10^{-6}$, SI); $P_J$, corrected anisotropy parameter; *L*, magnetic lineation; *F*; magnetic foliation; *T*, shape of the anisotropy ellipsoid.

| Fm | Site | Lat/Long | Height [m] | SC | | AMS fabric | | | | | |
|---|---|---|---|---|---|---|---|---|---|---|---|
| | | | | Dec [°] | Inc [°] | n | $k_m$ [ $\times 10^{-6}$(SI)] | $P_J$ | L | F | T |
| LL | JS2 | 31.56 S, 68.71W | 700 | 32 | 74 | 8 | 38.30 | 1.034 | 1.015 | 1.019 | 0.100 |
| | JS1 | 31.56 S, 68.71W | 703 | 32 | 74 | 9 | 82.40 | 1.028 | 1.013 | 1.015 | 0.093 |
| | JS4 | 31.56 S, 68.71W | 709 | 26 | 66 | 5 | 68.40 | 1.017 | 1.010 | 1.007 | −0.183 |
| | JS3 | 31.56 S, 68.71W | 712 | 26 | 66 | 6 | 75.40 | 1.026 | 1.019 | 1.005 | −0.563 |
| | JS6 | 31.57 S, 68.70 W | 825 | 30 | 81 | 10 | 86.10 | 1.038 | 1.006 | 1.029 | 0.659 |
| | JS5 | 31.57 S, 68.70 W | 829 | 30 | 81 | 10 | 84.40 | 1.036 | 1.004 | 1.029 | 0.743 |
| Z | JS7 | 31.56 S, 68.71W | 1000 | 30 | 81 | 6 | 28.50 | 1.072 | 1.052 | 1.017 | −0.495 |
| | JS8 | 31.56 S, 68.71W | 1004 | 30 | 81 | 7 | 5.16 | 1.115 | 1.040 | 1.071 | 0.268 |
| | JS9 | 31.56 S, 68.71W | 1025 | 30 | 81 | 6 | −6.55 | 1.044 | 1.003 | 1.036 | 0.825 |
| | JS10 | 31.56 S, 68.71W | 1030 | 30 | 81 | 9 | −4.05 | 1.107 | 1.043 | 1.060 | 0.157 |
| LF | JS11 | 31.91 S, 68.68 W | 1325 | 4 | 88 | 2 | −11.2 | – | – | – | – |
| | JS12 | 31.91 S, 68.68 W | 1360 | 4 | 88 | 5 | −7.18 | 1.033 | 1.016 | 1.017 | 0.007 |
| | JS13 | 31.91 S, 68.68 W | 1640 | 18 | 83 | 5 | 32.90 | 1.038 | 1.009 | 1.028 | 0.516 |
| | JS14 | 31.91 S, 68.68 W | 1715 | 4 | 89 | 5 | 4.09 | 1.218 | 1.086 | 1.121 | 0.162 |
| | JS15 | 31.91 S, 68.68 W | 1775 | 4 | 89 | 6 | 2.62 | 1.374 | 1.046 | 1.284 | 0.695 |
| | JS16 | 31.91 S, 68.68 W | 1785 | 4 | 89 | 6 | 11.00 | 1.058 | 1.014 | 1.041 | 0.476 |
| LS | JS17 | 31.91 S, 68.68 W | 1815 | 4 | 89 | 9 | 4.89 | 1.206 | 1.073 | 1.121 | 0.236 |
| | JS22 | 31.96 S, 68.68 W | 1950 | 230 | 65 | 5 | −5.93 | 1.030 | 1.014 | 1.016 | 0.055 |
| | JS23 | 31.96 S, 68.68 W | 1955 | 220 | 75 | 5 | −3.33 | 1.229 | 1.110 | 1.107 | −0.011 |
| SJ | JS18 | 31.94 S, 68.70 W | 2060 | 221 | 38 | 2 | 51.9 | – | – | – | – |
| | JS19 | 31.94 S, 68.70 W | 2060 | 228 | 50 | 8 | 67.80 | 1.019 | 1.010 | 1.009 | −0.082 |
| | JS20 | 31.94 S, 68.70 W | 2063 | 44 | 77 | 6 | 52.50 | 1.027 | 1.017 | 1.010 | −0.263 |
| | JS21 | 31.94 S, 68.70 W | 2063 | 44 | 77 | 2 | 44.5 | – | – | – | – |

| Fm | Site | Lat/Long | Height [m] | SC | | AARM fabric | | | | | |
|---|---|---|---|---|---|---|---|---|---|---|---|
| | | | | Dec [°] | Inc [°] | n | $k_a$[ $\times 10^{-6}$(SI)] | $P_J$ | L | F | T |
| LL | JS2 | 31.56 S, 68.71W | 700 | 32 | 74 | 5 | 232.0 | 1.066 | 1.029 | 1.036 | 0.105 |
| | JS6 | 31.57 S, 68.70W | 825 | 30 | 81 | 6 | 393.0 | 1.099 | 1.015 | 1.076 | 0.664 |
| Z | JS8 | 31.56 S, 68.71W | 1004 | 30 | 81 | 5 | 39.0 | 1.135 | 1.110 | 1.011 | −0.814 |
| | JS10 | 31.56 S, 68.71W | 1030 | 30 | 81 | 5 | 29.6 | 1.250 | 1.158 | 1.075 | −0.339 |
| LF | JS14 | 31.91 S, 68.68 W | 1715 | 4 | 89 | 5 | 95.4 | 1.212 | 1.030 | 1.162 | 0.672 |
| LS | JS17 | 31.91 S, 68.68 W | 1815 | 4 | 89 | 5 | 243.0 | 1.272 | 1.099 | 1.156 | 0.211 |
| | JS23 | 31.96 S, 68.68 W | 1955 | 220 | 75 | 6 | 66.9 | 1.229 | 1.160 | 1.051 | −0.497 |
| SJ | JS19 | 31.94 S, 68.70 W | 2060 | 228 | 50 | 5 | 253.0 | 1.153 | 1.019 | 1.119 | 0.709 |
| | JS20 | 31.94 S, 68.70 W | 2063 | 44 | 44 | 5 | 240.0 | 1.220 | 1.109 | 1.100 | −0.042 |

intermediate one.

The shape of the susceptibility ellipsoids is oblate for all sites from the La Flecha Formation (JS12 to JS16) and for most sites of the La Laja, Zonda and La Silla Formations (the exceptions are JS3, JS4, JS7 and JS23, Table 2). Both measured sites from the San Juan Formation are prolate.

The anisotropy of anhysteretic remanent magnetization (AARM) was measured in 9 sites (47 specimens) by applying a 100 mT-AC field ($H_{AC}$) with a 50 μT-DC bias field ($H_{DC}$) and following a 12-position protocol (AGICO, Inc., 2001). The standard linear range between anhysteretic remanence and the $H_{DC}$ field was estimated from some pilot samples (Appendix 3). The equipment used was an AGICO LDA-3A demagnetizer/AMU-1 anhysteretic magnetizer and a JR6 spinner magnetometer. Five to six specimens from nine representative sites from the five formations were selected for measurement of the remanence anisotropy ellipsoid, which were well-defined in most cases (Figs. 11 and 12). The mean anhysteretic susceptibility $\kappa_a$ spans between $2.96 \times 10^{-5}$ and $3.93 \times 10^{-4}$ SI (Table 2, Fig. 10g).

As shown by bulk susceptibility values and hysteresis cycles (Fig. 8 and Appendix 2) paramagnetic signal dominates all samples from the La Laja Formation, while three out of four samples from the Zonda Formation and one sample (JS23-4a) from the La Silla Formation (Fig. 8 and Appendix 2) present a dominant diamagnetic character. All samples from the La Flecha, and San Juan Formations, plus site JS17 from La Silla Formation show a dominantly ferromagnetic (*s.l.*) character (see Appendix 2). Thus, it is expected that the source of magnetic anisotropy is mainly governed by: paramagnetic fractions in samples from the La Laja Formation, diamagnetic ones in most samples from the Zonda Formation and in some samples from the La Silla Formation and ferromagnetic minerals, in all samples from the La Flecha and San Juan Formations as well as some samples from the La Silla Formation.

In general, remanence and susceptibility fabrics are consistent in all analysed sites. Directions of principal axes do not vary or vary slightly at each site. Only the ellipsoidal shape shows some differences in three out of nine cases. The AMS ellipsoidal shape for sites JS8 and JS10 is slightly oblate, while the AARM ellipsoid is prolate (Table 2). Meanwhile JS19 (San Juan Formation) shows a prolate (almost triaxial) AMS fabric and a well-defined oblate AARM ellipsoid. Both the shape and orientation of the AARM ellipsoids are consistent with those of the AMS in the other six (out of nine) measured sites (JS2, JS6, JS14, JS17, JS20 and JS23, Table 2).

The lowest mean magnetic susceptibility corrected anisotropy degree ($P_J$) per geologic unit (Table 2) is found in the San Juan Formation with 1.023, followed by the La Laja Formation with 1.030,

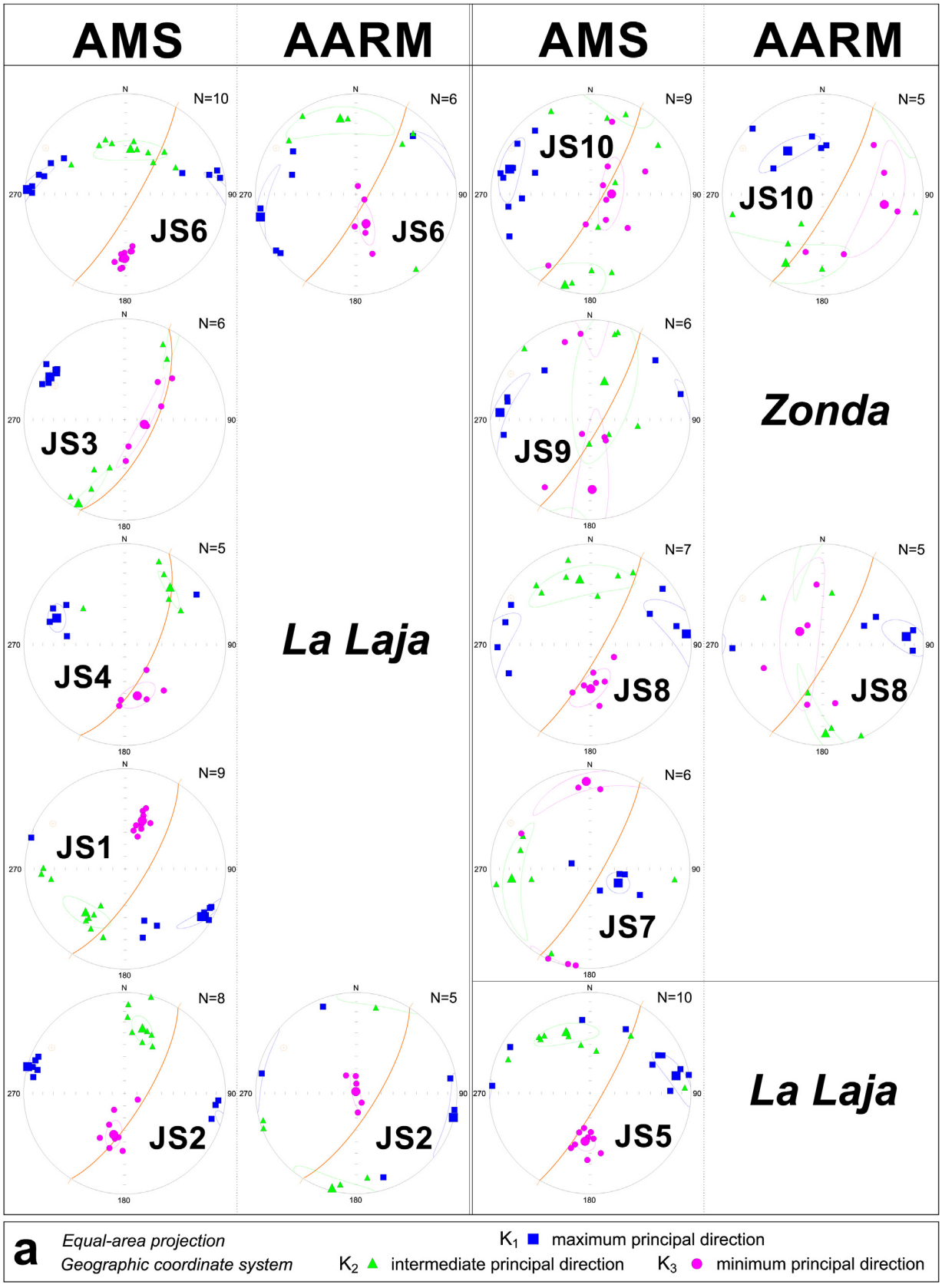


**Fig. 11.** Principal directions of the anisotropy of magnetic susceptibility (AMS) and the anisotropy of anhysteretic remanent magnetization (AARM) fabrics in equal-area projections (lower hemisphere), in the geographic coordinate system, for sites along the sequence. The ellipses correspond to 95% confidence regions about the mean axes (Jelínek, 1978). Projections of the bedding plane and pole to the bedding are shown (orange). **a)** Sites unaffected by the Sanrafaelic overprint. **b)** Sites affected by the Sanrafaelic remagnetization. (For interpretation of the references to colour in this figure legend, the reader is referred to the web version of this article.)

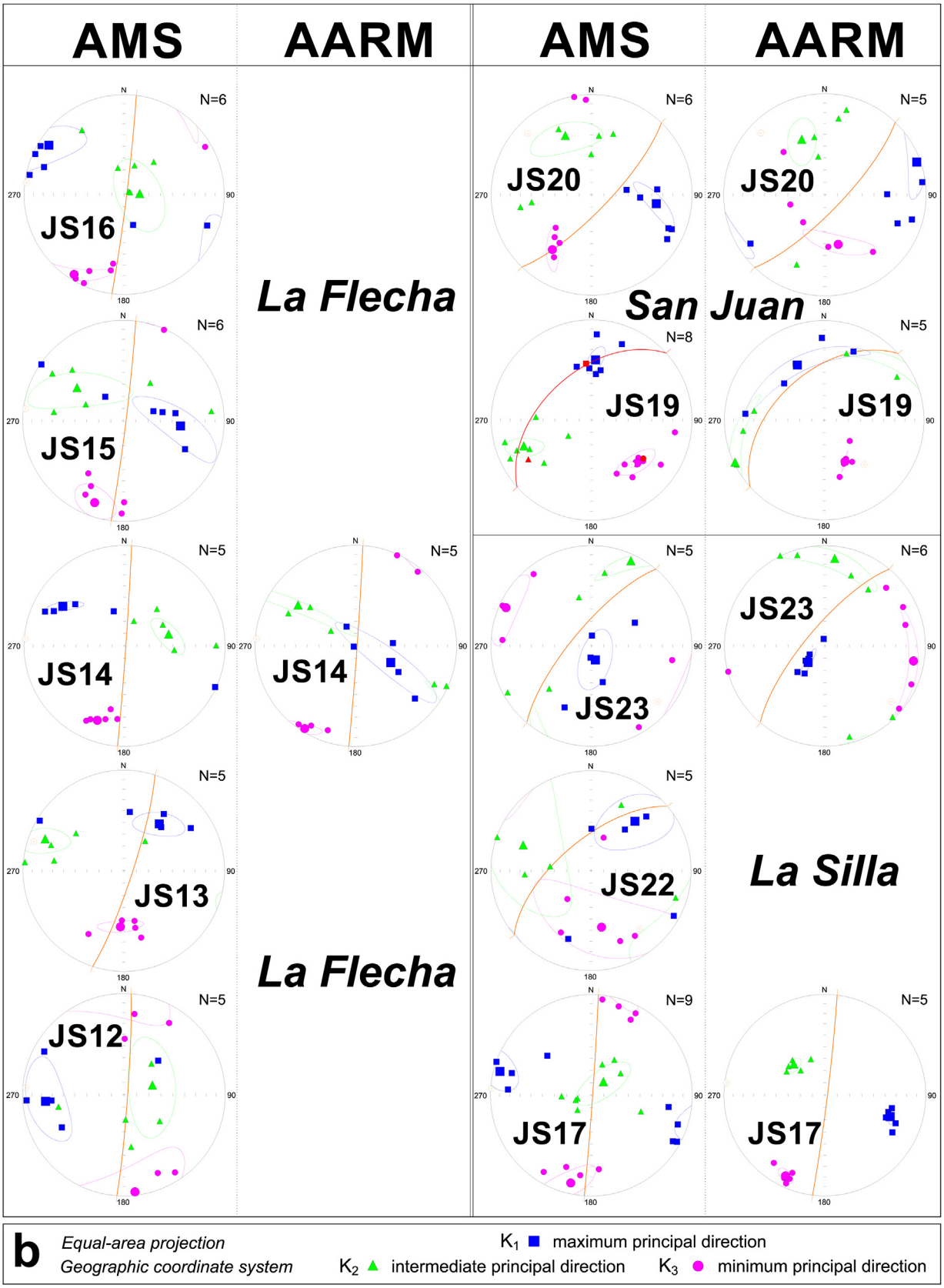


**Fig. 11.** (*continued*).

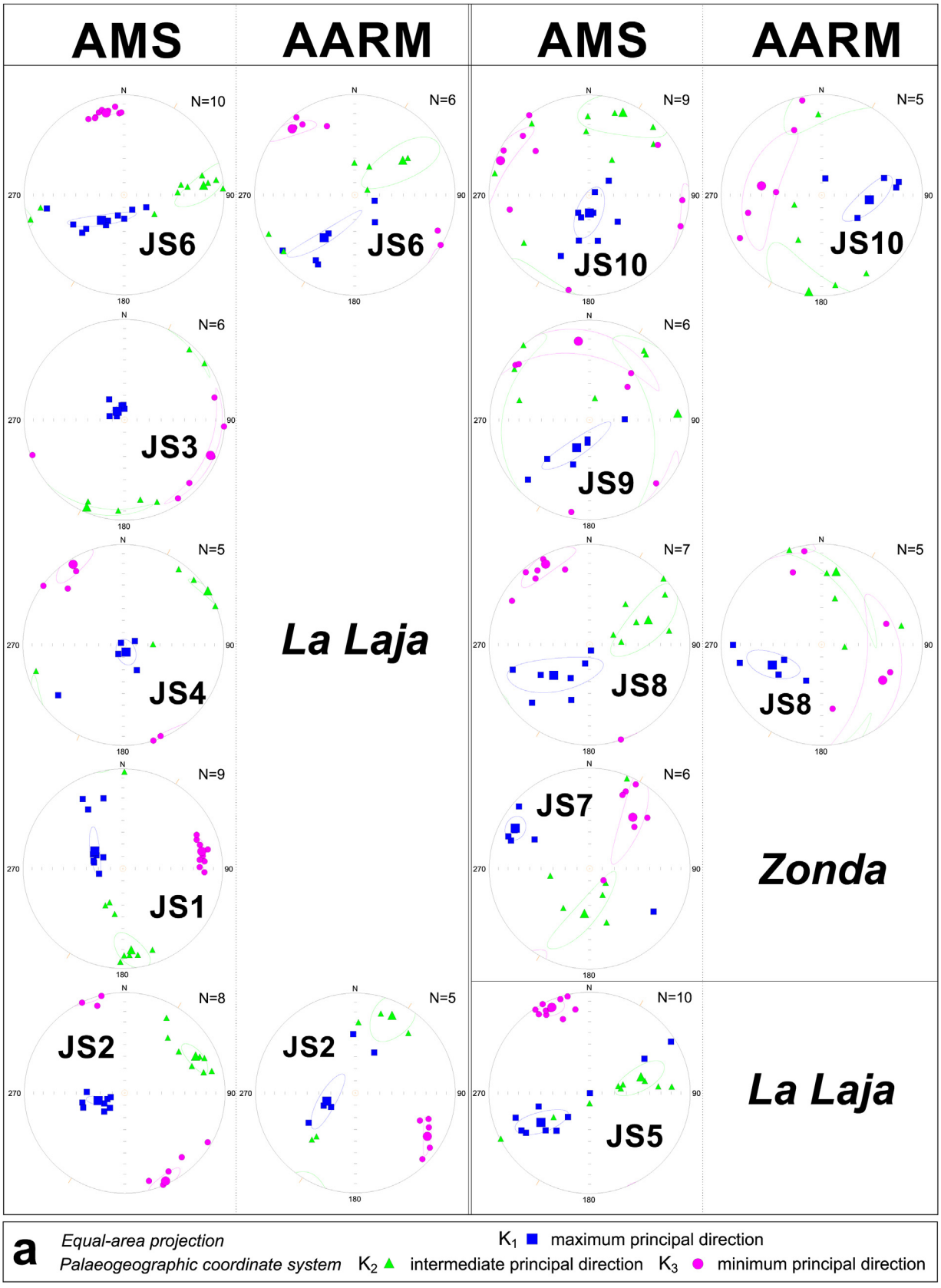


**Fig. 12.** Principal directions of the anisotropy of magnetic susceptibility (AMS) and the anisotropy of anhysteretic remanent magnetization (AARM) fabrics in equal-area projections (lower hemisphere), in the palaeogeographic coordinate system, for sites along the sequence. The ellipses correspond to 95% confidence regions about the mean axes (Jelínek, 1978). Projection of pole to the bedding is shown (orange). **a)** Sites unaffected by the Sanrafaelic overprint. **b)** Sites affected by the Sanrafaelic remagnetization. (For interpretation of the references to colour in this figure legend, the reader is referred to the web version of this article.)

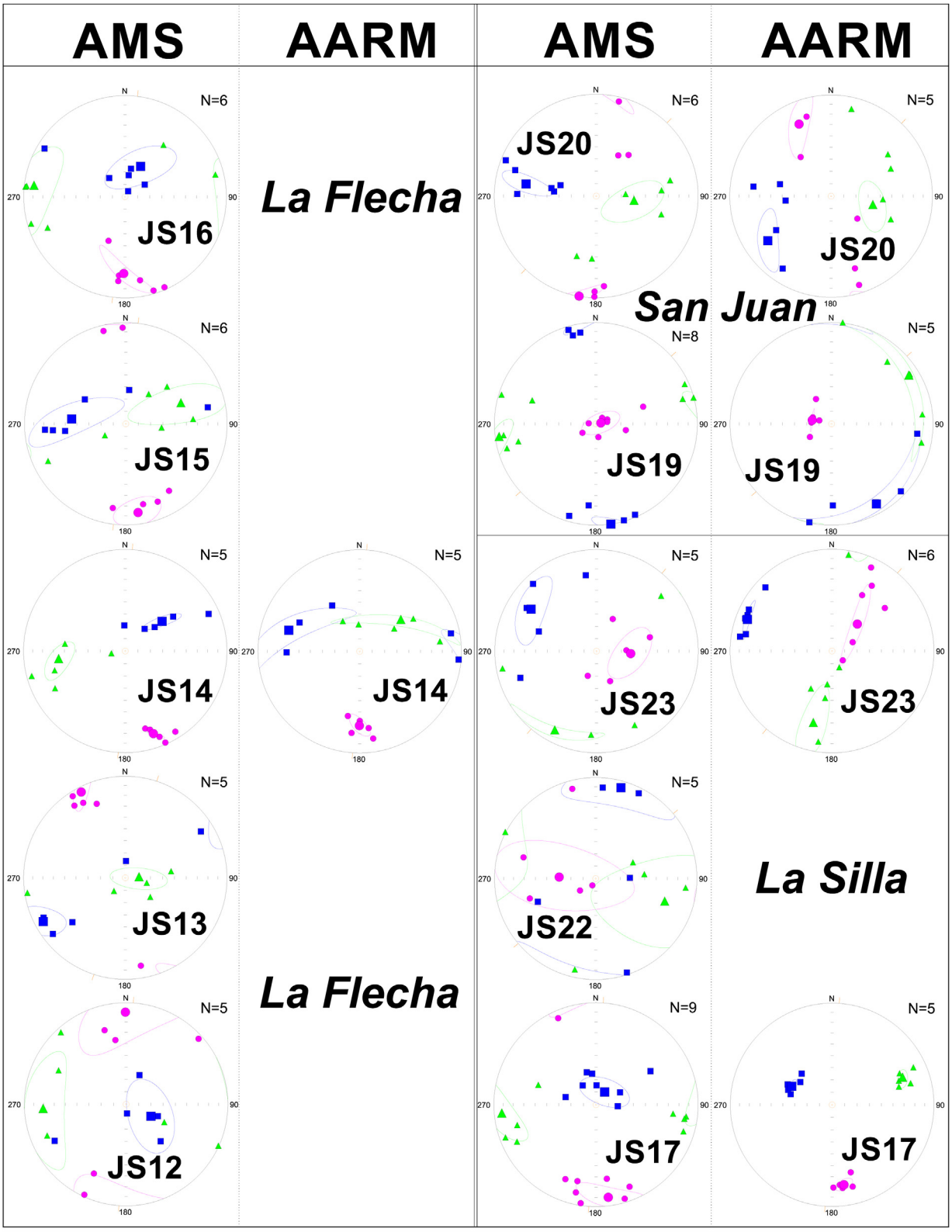


**Fig. 12.** (*continued*).

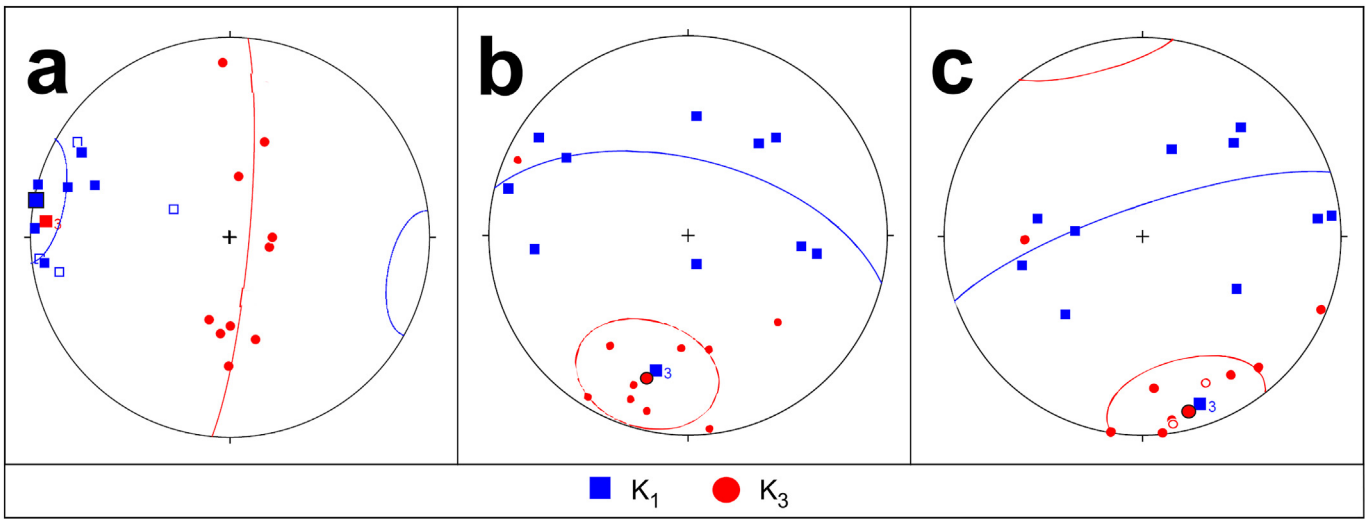


**Fig. 13.** **a)** Site-mean $K_1$ and $K_3$ axes for units unaffected by the Sanrafaelic remagnetization (La Laja and Zonda Formations), *in situ*. Site-mean $K_1$ and $K_3$ axes for the carbonate units affected by the Sanrafaelic remagnetization (La Flecha, La Silla and San Juan Formations) **(b)** *in situ* and **(c)** after correction for the rotation proposed by Rapalini et al. (2000) for the Neogene uplift of the Eastern Precordillera. Stereoplots are in equal-area projections (lower hemisphere). The 95% confidence regions about the mean axes and best fit great circles are shown. Poles to the planes are indicated by (3). Mean axes and cones of uncertainty were estimated by Fisher statistics over the site-means. Girdle distributions were analysed by Bingham statistics (Mardia, 1972).

the Zonda Formation with 1.085, the La Flecha Formation with 1.144 and, finally, the La Silla Formation, with 1.155. In the case of the anhysteretic remanence fabrics, the lowest corrected anisotropy degree is found in the La Laja Formation, with 1.083. It is followed by the San Juan, Zonda, La Flecha and La Silla Formations, with values of 1.186, 1.193, 1.212 and 1.251, respectively. This illustrates that the anisotropy degree follows similar patterns in all formations for both the AMS and AARM measurements. As it is expected, the latter tend to be significantly higher than the former.

### 4.3. X-ray diffraction analyses

Analysis by X-ray Diffraction (XRD) was carried out by operating a PANalytical X'Pert Pro diffractometer at 40 kV and 40 mA with a Cu Kα source ($\lambda = 1.5403$ Å) in 13 representative samples covering the whole sequence. Two samples from La Laja Formation (JS2-2 from the Rivadavia Member and JS6-6 from the Juan Pobre Member), two samples from the Zonda Formation (JS8-4 and JS10-2), three samples from the La Flecha Formation (JS12-3, JS14-6 and JS16-2), three samples from the La Silla Formation (JS17-1, JS22-2 and JS23-1) and three samples from the San Juan Formation (JS18-4, JS19-4 and JS20-1) were selected for X-ray diffraction analyses. The main goal was to determine the amount and type of clay minerals present in the analysed succession. General results indicate calcite as the dominant mineralogical fraction in most samples, with variable presence of dolomite, which becomes dominant in a couple of samples from the Zonda Formation. Quartz appears also in variable quantities but always as a very minor component. Concerning the clay minerals, the analyses indicate that they are virtually absent in the whole succession. In all cases their presence is under 1%. In particular, no traces of illite were found in any of the thirteen analysed samples.

## 5. Discussion

The highest content of $MgCO_3$, above 30% (Fig. 10b and c) is found in the central portion of the studied succession, throughout the upper part of the Juan Pobre Member (La Laja Formation), in the entire Zonda Formation and all through the La Flecha Formation, according to the comprehensive studies of Bordonaro (2002). Very low mean magnetic susceptibility values, including negative magnitudes, were found at these levels. In the Zonda Formation, three out four samples (sites JS7, JS8 and JS9) show hysteresis loops with a strong diamagnetic contribution. In particular, more than 40% of $MgCO_3$ was reported for this unit. On the contrary, sites that are located in layers that are characterized by the greatest ratio of $CaCO_3$ (JS1 to JS6 and JS18 to JS21, i.e. those from the Rivadavia Member of the La Laja Formation and from the San Juan Formation), present the highest values of $\kappa_m$ (Table 2). It appears, therefore, that dolomitization inversely correlates with several magnetic properties, particularly bulk susceptibility and NRM intensity (Fig. 10). The presence of finely laminated dolomite levels in the La Silla Formation have been described by Raviolo et al. (2007, 2009). Pratt et al. (2011) reported that it is non-ferroan dolomite. Consistently, sites JS22 and JS23 from that formation show negative bulk susceptibility values (Table 2). Hysteresis loops from sites JS1 to JS6 (Rivadavia Member of the La Laja Formation) present a distinct paramagnetic contribution and an "inverse" magnetic fabric which may probably be related to iron-bearing limestones (see Borradaile and Jackson, 2010), as according to Bordonaro (2002) this member is characterized by over 90% of calcium carbonate, no significant magnesium contribution and negligible insoluble residues (<2%). On the other hand, San Juan Formation samples also are devoid of significant contribution of dolomite, but contrary to the La Laja Formation rocks, its hysteresis cycles show a clear dominance of ferromagnetic fractions.

Rapalini et al. (2000) found that the Sanrafaelic remagnetization

was only carried by the La Flecha, La Silla and San Juan Formations, and not by the lowest units of the succession (La Laja and Zonda Formations). This indicates that, although a clear stratigraphic control on many magnetic parameters is observed, dolomitization is not related to the remagnetization process nor it has conditioned its occurrence. Though magnesium carbonate is present at very low rates (or absent) in the La Laja and in the San Juan Formations, the former unit does not carry the Permian remagnetization, while the latter does it. In fact, Gómez and Astini (2006) stated that the highly developed dolomitization in the upper portion of the Zonda Formation is most probably the result of an early diagenetic process. Raviolo et al. (2009) reached similar conclusions for the dolomite levels of the La Silla Formation. This points towards a secondary origin for the carriers of the Sanrafaelic remanence, and probably also of the recent magnetization. The chemical origin of the remagnetization is also supported by some significantly different magnetic properties found in those units affected by the late Palaeozoic event and those only affected by the recent overprint. The La Laja Formation, with no evidence of the ancient remagnetization, is characterized by hysteresis cycles dominated by paramagnetic fractions (probably Fe-bearing limestones), while hysteresis cycles from the San Juan and La Flecha Formations are basically ferromagnetic. The "ferromagnetic" cycles (see Appendix 2) seem to be a "fingerprint" of carbonates remagnetized by the Sanrafaelic event in this succession. This is more easily explained by neo-mineral formation processes associated with this event, as it has been found to be the case in the Ponón Trehué limestones of the San Rafael Block (Fazzito and Rapalini, 2016).

The magnetic fabrics also point to significant differences between the rocks that carry the late Palaeozoic remagnetization and those that do not. Fig. 13a shows the distribution of site-mean $K_1$ and $K_3$ axes for the La Laja and Zonda Formations, which do not carry the Sanrafaelic overprint. A "prolate" overall distribution of AMS axes is clearly shown with subhorizontal $K_1$ axes pointing west and a subvertical girdle of $K_3$ axes in *in situ* coordinates. The AARM data obtained do not show significant differences. On the other hand, site-mean $K_1$ and $K_3$ axes for the carbonates of the La Flecha, La Silla and San Juan Formations, that carry the late Palaeozoic remagnetization, show an "oblate" distribution (Fig. 13b) with shallow AMS $K_3$ axes pointing SSW and a girdle of $K_1$ axes dipping at high angle towards the NNE. Rapalini et al. (2000) interpreted that the Sanrafaelic remagnetization was affected by tilting due to Andean uplift of the Eastern Precordillera. They suggested a 40° ccw rotation around an axis plunging 30° to N30°E which is compatible with structural models of back-thrust thick-skinned deformation of the Eastern Precordillera, bedding attitudes of late Tertiary sediments in the area and the restoration of the remanence direction to an expected Permian position. If this rotation for the Neogene uplift of the Eastern Precordillera is applied to these data (Fig. 13c), a nearly subhorizontal south pointing $K_3$ axes and a subvertical E-W magnetic foliation are obtained. The AARM ellipsoids do not differ significantly from those of the AMS, strongly suggesting that the AMS ellipsoids are a good approximation to the fabric of the remanence carriers. Since the magnetic fabric pattern of the section carrying the Sanrafaelic magnetization (La Flecha, La Silla and San Juan Formations) is significantly different from that of the lower section (La Laja and Zonda Formations) that only shows a recent magnetization, it looks very likely that this is due to different mineral assemblages produced at different times. Otherwise, we would expect similar fabrics or at least not systematically different ones. In brief, the simplest explanation is that new magnetic minerals formed in the lower section in Recent times with such new fabrics rather than an older mineral assemblage (like that carrying the Permian magnetization) that was reset by viscous processes. Whether the partial recent overprint (Component A) of the upper section is viscous or chemical remains unclear, although the rock magnetic experiments described above together with the unblocking temperature of this component are suggestive of pyrrhotite as the likely carrier. This would point to a chemical origin too for the recent component in these rocks. NRM representative demagnetization curves for samples of the whole collection do not show significant differences in coercivity spectra between those samples carrying the Sanrafaelic remagnetization and those that do not (Appendix 4), suggesting that the latter do not appear as more prone to acquire a viscous magnetization than the former.

Multiple rock magnetic experiments and analyses, described above, show that the carbonate succession of the Eastern Precordillera carries a complex and variable ferromagnetic (*s.l.*) mineral assembly. The La Laja Formation shows the presence of significant goethite, (Ti?) magnetite and variable amounts of haematite (see Fig. 5) with minimum or no traces of pyrrhotite. The recent magnetization found in these rocks show moderate coercivity spectra and unblocking temperatures between 350 °C and 500 °C (Fig. 2) indicating that titanomagnetite is the most likely carrier of this remanence, and besides its apparent significance in some Lowrie demagnetization tests, haematite is not a main contributor to the natural remanence. The Zonda Formation, despite carrying the same remanence, do not show significant goethite, shows the apparent presence of pyrrhotite (Fig. 5) and (Ti?) magnetite, with very variable presence of haematite. Unblocking temperatures of 350–450 °C (Fig. 2) suggest that magnetite (and possibly pyrrhotite) carry the secondary remanence, with no significant evidence of haematite as its carrier. This suggests that (Ti?) magnetite and possibly pyrrhotite of secondary origin carry the recent remagnetization found in those formations.

The Sanrafaelic overprint is characterized by a magnetic component unblocked between 350 °C and 500–550 °C, which tied with some rock magnetic results, strongly suggest that it is carried exclusively by magnetite (Fig. 2). Most samples that carry this component also show the presence of a lower-temperature (<350 °C) magnetic component. Rapalini et al. (2000) demonstrated that this low-temperature overprint is recent due to its exclusive normal polarity and coincidence with the Dipole Field direction. It is also coincident with the remanence isolated at the La Laja and Zonda Formations, suggesting that it may have been produced by the same process. In the La Flecha, La Silla and San Juan Formations, this recent overprint did not erase completely the Sanrafaelic remagnetization. Whether the La Laja and Zonda Formations ever had that magnetization cannot be known with the available information. A large mineral variability is also observed in the carbonates remagnetized by the Sanrafaelic event. Magnetite is undoubtedly the main carrier of this component, while the partial overprint is probably carried by pyrrhotite (and titanomagnetite?). Goethite seems to be absent or in negligible quantities, suggesting that unsaturated IRM acquisition curves (Fig. 4) are due to the presence of haematite. This appears in very different quantities in different samples, from dominating the 3D-IRM demagnetization plots (JS11-5a from the La Flecha Formation and JS19-4b from the San Juan Formation, Fig. 5) to being absent (JS12-2 and JS14-4 from the La Flecha Formation and JS17-4c from the La Silla Formation, Fig. 5). In any case, its influence in the NRM demagnetization behaviour seems minor to negligible as shown by the unblocking temperatures already mentioned (Fig. 2). Frequent drops in the 3D-IRM demagnetization plots of all coercivity fractions around 300 °C

point towards the presence of pyrrhotite in several samples which is therefore the most likely carrier of the recent overprint in these sites.

Rapalini and Astini (2005) suggested that the Sanrafaelic regional remagnetization was due to chemically active fluids expelled from the San Rafael Orogen towards the foreland producing a diachronic remagnetization, in which rocks located eastwards were remagnetized somewhat later. Fazzito and Rapalini (2016) have proposed that the "orogenic fluids" hypothesis is a viable one for the remagnetized Ponón Trehué Formation, although hydrothermal fluids associated to the Choiyoi magmatism cannot be ruled out yet. Ramos and Folguera (2009) proposed that the Sanrafaelic remagnetization was associated to an anomalous regional increase in heat flow preceding the development of the large Choiyoi igneous province. Whether that anomalous heat flow produced hydrothermal fluids that affected the Eastern Precordillera leading to chemical precipitation of magnetite is not clear, but the magnetic characteristics of the carbonates under study rule out a remagnetization of thermoviscous origin. No late Palaeozoic magmatic rocks are exposed in the Eastern Precordillera or nearby which suggests that remagnetization due to hydrothermal fluids affecting the carbonates is unlikely.

Katz et al. (2000) proposed that regional remagnetizations can be produced by burial diagenesis and chemical alteration of clays, in particular transformation of smectite into illite producing secondary magnetite. Fazzito and Rapalini (2016) ruled out this mechanism for the Sanrafaelic remagnetization in the Ponón Trehué area, mainly based in the fact that at such locality the remagnetization is carried by both magnetite and pyrrhotite. This seems not the case in the Eastern Precordillera, where the Sanrafaelic overprint is only carried by magnetite. Our XRD analyses demonstrate, however, that clay minerals are only traces (<1%) in all samples, regardless their stratigraphic position and whether or not they carry the late Palaeozoic overprint. Even more, not even traces of illite were found in any of the samples. These results strongly suggest that the burial transformation of clays is not a viable explanation for the Sanrafaelic remagnetization.

The previous discussion and the pattern of a younger remanence towards the foreland of the San Rafael Orogen indicated by Rapalini and Astini (2005), suggest that the original proposal that the regional Sanrafaelic remagnetization was caused by chemically active fluids expelled from the orogen (e.g. Oliver, 1986) during this major tectonic event, still holds as a viable explanation.

## 6. Conclusions

A systematic rock magnetic and magnetic fabric study was carried out on samples from twenty-three sites along the middle Cambrian to early Ordovician carbonate platform of the Eastern Precordillera of Argentina. This succession comprises the La Laja, Zonda, La Flecha, La Silla and San Juan Formations. A previous study had shown that the latter three carry a late Palaeozoic magnetic overprint known as the "Sanrafaelic remagnetization", while the former two do not and are carriers of a recent overprint. Different rock magnetic parameters show a stratigraphic (lithologic) correlation that is particularly strong with the early diagenetic dolomitization of the sequence. However, this does not correlate with the presence or absence of the overprints, suggesting that both are due to secondary formation of the magnetic carriers. A complex magnetic mineralogy is evident from the results of this study in all formations. In spite of this, solely magnetite seems to carry the Sanrafaelic overprint meanwhile pyrrhotite and/or (Ti?) magnetite would carry the recent magnetization.

A clear correlation pattern, however, has been found in the character of the hysteresis loops which are governed by paramagnetic or diamagnetic fractions in the recently remagnetized rocks while they are dominated by ferromagnetic fractions in those affected by the late Palaeozoic overprint.

Magnetic fabrics studied through AMS and AARM show similar patterns with both properties, indicating that the ferromagnetic fabric does not differ significantly from the overall magnetic one, and may actually be controlling it. However, a clearly different directional pattern is observed between rocks affected by the Sanrafaelic overprint and those that are not, suggesting independent processes of fabric formation and supporting an independent chemical origin for both overprints.

X-ray diffraction results indicate that clay minerals are virtually absent in all analysed rocks and no traces of illite have been found, ruling out the burial diagenesis of clay minerals for the origin of the Sanrafaelic remagnetization. Lack of exposed late Palaeozoic magmatic units in the Eastern Precordillera turns unlikely a remagnetization related to hydrothermal fluids too. The originally proposed model of the Sanrafaelic remagnetization as produced by chemically active fluids, expelled from the San Rafael Orogen towards the foreland, still holds as the most likely explanation for this widespread geologic event.

## Acknowledgements

We are deeply grateful to Thelma S. Berquó for measurements of thermomagnetic curves and hysteresis loops at the Instituto Astronômico e Geofísico (Universidade do São Paulo, Brazil). Technical support by Carlos Vasquez and Matías Naselli are sincerely thanked. Fernando Almaraz kindly collaborated in the preparation of rocks for XRD studies. We are indebted to Germán S. Kürten Moreno for operating the X-ray diffractometer at Centro de Investigaciones Geológicas (CIG, Universidad Nacional de La Plata). Measurements by means of the ASC Scientific IM-10-30 pulse magnetizer, the ASC Scientific TD 48 SC furnace, the AGICO JR6 Spinner magnetometer, the AGICO Multi-function Kappabridge susceptibility-metre and the AGICO LDA-3A demagnetizer/AMU-1 anhysteretic magnetizer were conducted at Laboratorio de Paleomagnetismo Daniel A. Valencio (IGEBA, Universidad de Buenos Aires). Anisotropy and remanence tensors were analysed by Jelínek (1978) statistics by using the Anisoft 4.2 software (AGICO, Inc.). Statistical analysis of principal directions of magnetic susceptibility over units with/without the Sanrafaelic overprint was carried out with the help of Stereonet 9.5 (Allmendinger et al., 2012; Cardozo and Allmendinger, 2013). Financial support for this research was provided by Agencia Nacional de Promoción Científica y Tecnológica (PICT-2011-0956 and PICT-2014-1516 grants) and Universidad de Buenos Aires (UBACyT 20020130100465BA). We greatly appreciate the suggestions from two anonymous reviewers who helped us to improve the manuscript. This paper is dedicated to the memory of our dear and remarkable colleague Dr. Rubén Somoza.

## Appendix 1

More examples of thermal decay of triaxial IRM plots from the La Flecha, La Silla and San Juan Formations. Insets show curves normalized by the maximum intensity of the coercivity fraction.

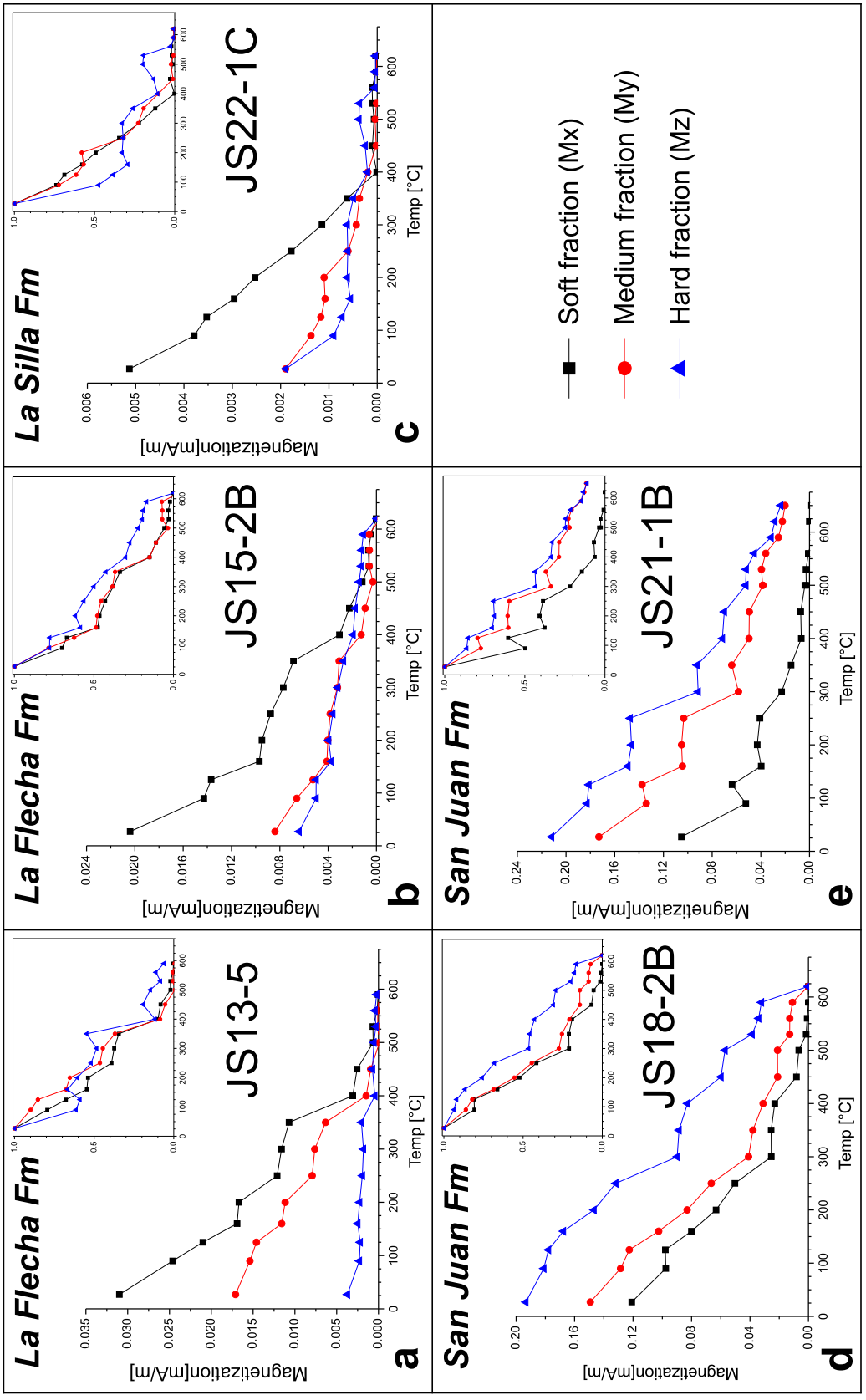
La Flecha Fm
JS13-5
a
La Flecha Fm
JS15-2B
b
La Silla Fm
JS22-1C
c
San Juan Fm
JS18-2B
d
San Juan Fm
JS21-1B
e
Magnetization[mA/m]
Temp [°C]
Soft fraction (Mx)
Medium fraction (My)
Hard fraction (Mz)

**Appendix 2**

The complete set of hysteresis loops obtained from the 23 palaeomagnetic sites, before (green) and after (blue) subtraction of diamagnetic or paramagnetic high-field slope. Red dashed line: smoothed curve.

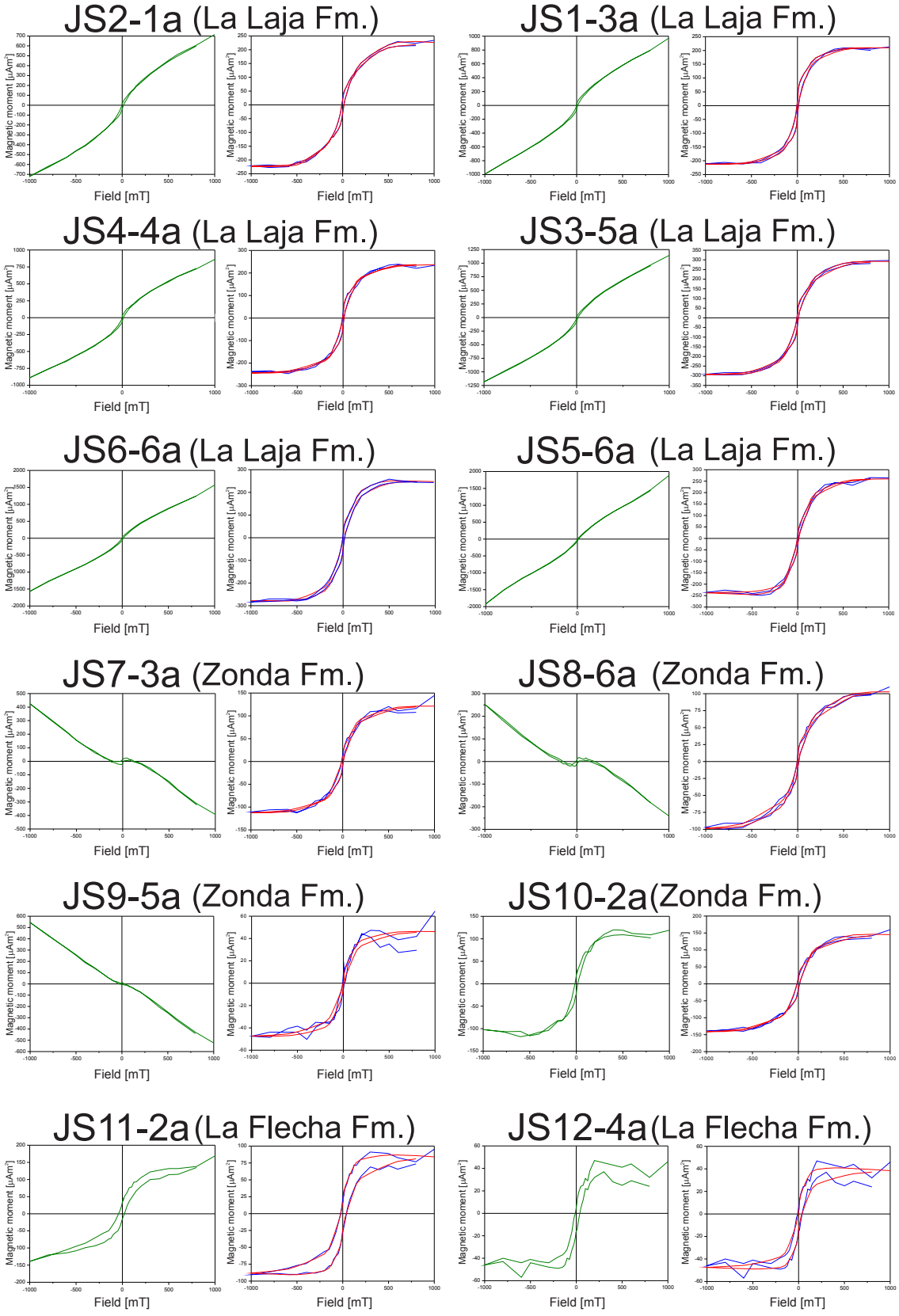

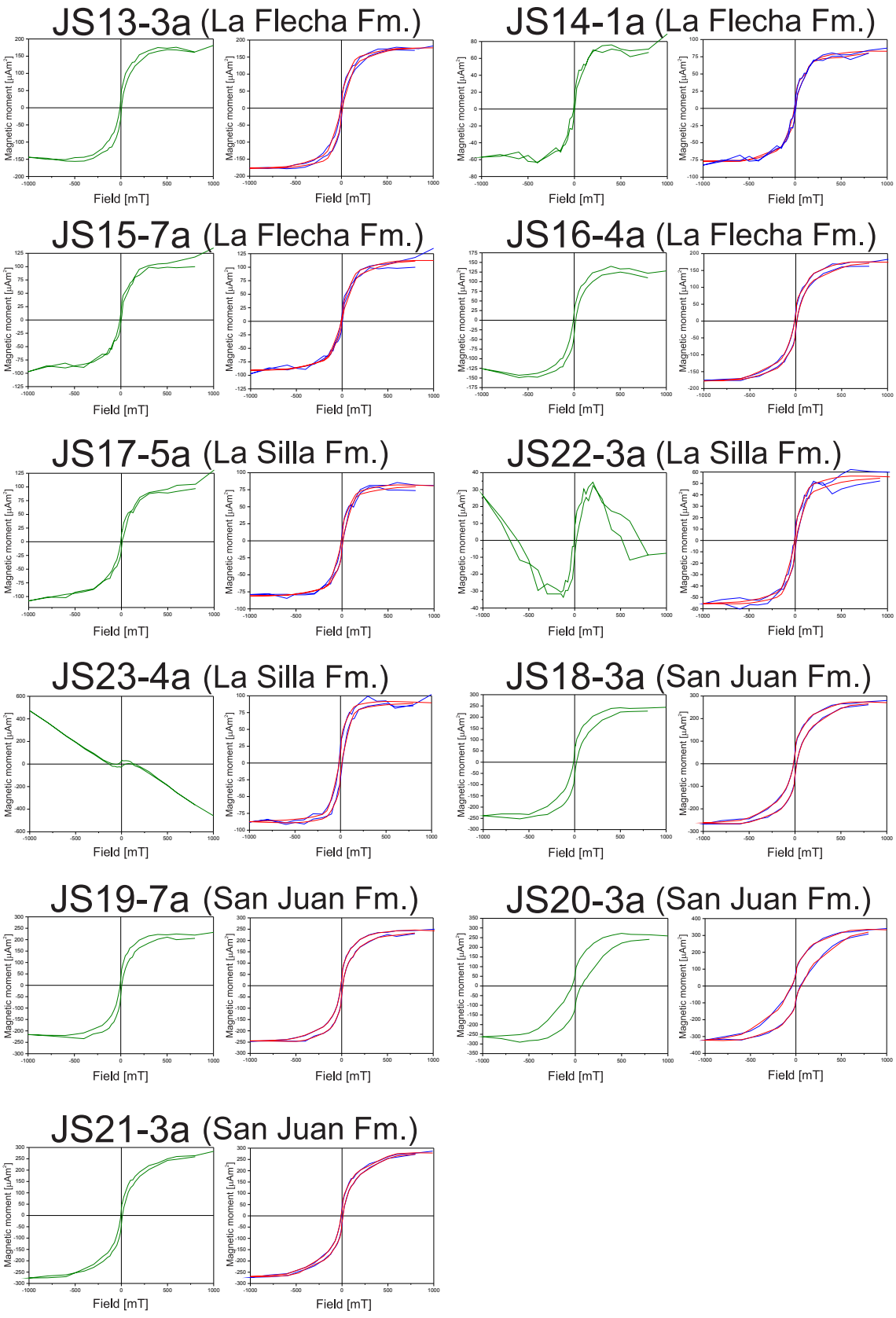
JS13-3a (La Flecha Fm.)
JS14-1a (La Flecha Fm.)
JS15-7a (La Flecha Fm.)
JS16-4a (La Flecha Fm.)
JS17-5a (La Silla Fm.)
JS22-3a (La Silla Fm.)
JS23-4a (La Silla Fm.)
JS18-3a (San Juan Fm.)
JS19-7a (San Juan Fm.)
JS20-3a (San Juan Fm.)
JS21-3a (San Juan Fm.)
Magnetic moment [μAm²]
Field [mT]

## Appendix 3

Some examples of anhysteretic remanent magnetization curves acquired in DC bias fields up to 500 μT with an AC field of 100 mT. A linear behaviour is observed at low direct fields (typically ≤ 50 μT).

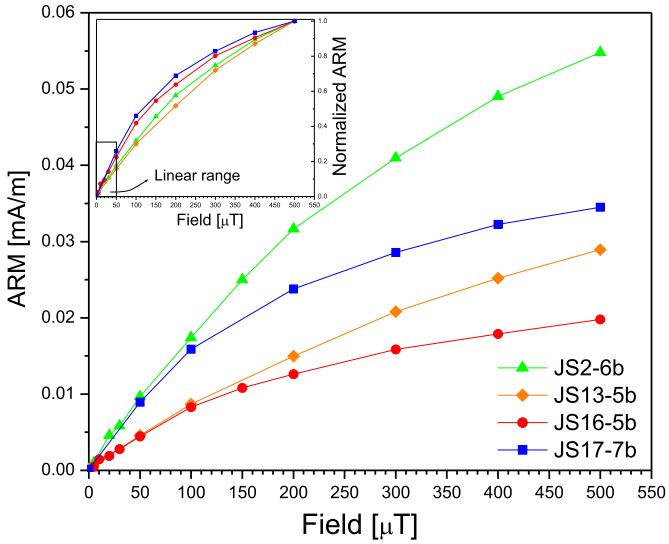


## Appendix 4

Magnetic intensity decay of samples from units with Sanrafaelic remagnetization (blue lines) and from units without Sanrafaelic remagnetization (red dashed lines) during AF stepwise demagnetization treatment.

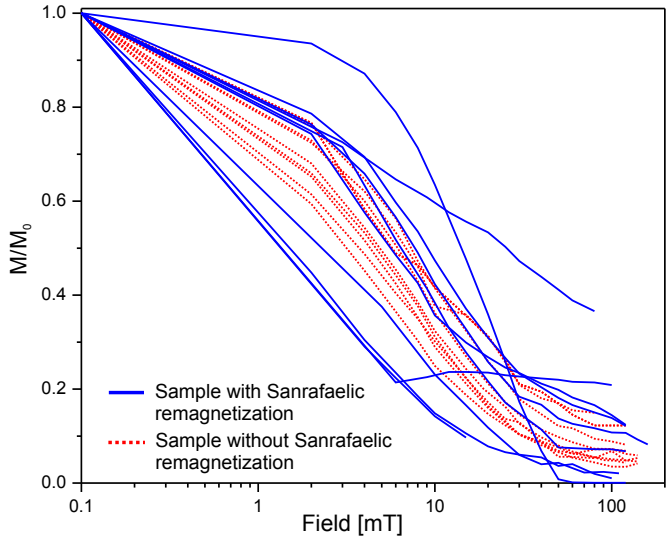


## References


AGICO, Inc., 2001. LDA-3A AF Demagnetizer and AMU-1A Anhysteretic Magnetizer. User's Guide. Print No. 32, ver. 5 available at: www.agico.com.

Allmendinger, R.W., Cardozo, N.C., Fisher, D., 2012. Structural Geology Algorithms: Vectors and Tensors. Cambridge University Press, Cambridge, England, p. 289.

Arroqui Langer, A., Bordonaro, O., Chávez, I., 2006. Aplicación de un patrón de exploración y explotación en la minería de carbonatos, en el ámbito de la Precordillera Argentina. Bol. Geol. Min. 117 (4), 649–654.

Astini, R.A., Ramos, V.A., Benedetto, J.L., Vaccari, N.E., Cañas, F.L., 1996. La Precordillera: un terreno exótico a Gondwana. In: XIII Congreso Geológico Argentino y III Congreso de Exploración de Hidrocarburos, Buenos Aires, Actas, vol. 5, pp. 293–324.

Astini, R.A., Benedetto, J.L., Vaccari, N.E., 1995. The early Paleozoic evolution of the Argentine Precordillera as a Laurentian rifted, drifted and collided terrane: a geodynamic model. Geol. Soc. Am. Bull. Geol. Soc. Am. Bull. 107 (3), 253–273.

Azcuy, C.L., Caminos, R., 1987. Diastrofismo. In: Archangelsky, S. (Ed.), El Sistema Carbonífero en la República Argentina. Academia Nacional de Ciencias Córdoba, Córdoba, pp. 239–252.

Baldis, B., Bordonaro, O., 1981. Evolución de facies carbonáticas en la cuenca cámbrica de la Precordillera de San Juan. In: VIII Congreso Geológico Argentino, San Luis, Actas, vol. 2, pp. 385–397.

Baldis, B., Bordonaro, O., 1984. Cámbrico y Ordovícico en la Sierra Chica de Zonda y Cerro Pedernal, provincia de San Juan. Génesis del margen continental en la Precordillera. In: IX Congreso Geológico Argentino, San Carlos de Bariloche, Argentina, Actas, vol. 4, pp. 190–207.

Baldis, B.A., Beresi, M.S., Bordonaro, O., Vaca, A., 1982. Síntesis evolutiva de la Precordillera argentina In: V Congr. Latinoam. Geol., 4, 399–441.

Baldis, B., Beresi, M., Bordonaro, O., Vaca, A., 1984. The argentine Precordillera as a key to andean structure. Episodes 7 (3), 14–19.

Benedetto, J.L., 2004. The allochthony of the Argentine Precordillera ten years later (1993-2003): a new paleobiogeographic test of the microcontinental model. Gondwana Res. 7 (4), 1027–1039.

Benedetto, J.L., Carrera, M.G., Sánchez, T.M., 1995. The evolution of faunal provincialism in the Argentine Precordillera during the Ordovician: new evidence and paleontological implications. In: Cooper, J.D., Droser, M.L., Finney, S.C. (Eds.), Ordovician Odyssey-Pacific Section, Book 77. Society of Economic Paleontologists and Mineralogists, Tulsa, OK, pp. 181–184.

Bordonaro, O., 1980. El Cámbrico en la Quebrada de Zonda. Prov. San Juan. Rev. Asoc. Geol. Arg 35 (1), 26–40.

Bordonaro, O., 1983. El factor estratigráfico como control en la prospección de calizas y dolomías en la Sierra Chica de Zonda, San Juan. In: II Congreso Argentino de Geología Económica, San Juan, Actas, vol. 1, pp. 193–203.

Bordonaro, O.L., 2002. Industrial use of the cambrian and ordovician carbonatic rocks from the argentine. In: Trombotto, D., Villalba, R. (Eds.), IANIGLA, 30 Years of Basic and Applied Research on Environmental Science, pp. 123–126.

Bordonaro, O.L., 2003a. Review of the cambrian stratigraphy of the argentine Precordillera. Geol. Acta 1 (1), 11–21.

Bordonaro, O.L., 2003b. Evolución paleoambiental y paleogeográfica de la cuenca cámbrica de la Precordillera Argentina. Rev. Asoc. Geol. Arg. 58 (3), 329–346.

Borradaile, G.J., Almqvist, B.S.G., Geneviciene, I., 2012. Anisotropy of magnetic susceptibility (AMS) and diamagnetic fabrics in the Durness Limestone, NW Scotland. J. Struct. Geol. 34, 54–60. http://dx.doi.org/10.1016/j.jsg.2011.10.008.

Borradaile, G.J., Jackson, M., 2010. Structural geology, petrofabrics and magnetic fabrics (AMS, AARM, AIRM). J. Struct. Geol. 32, 1519–1551.

Cardozo, N., Allmendinger, R.W., 2013. Spherical projections with OSXStereonet. Comput. Geosci. 51, 193–205.

Cisowski, S., 1981. Interacting vs. non-interacting single domain behavior in natural and synthetic samples. Phys. Earth Planet. Inter 26 (1–2), 56–62.

Channell, J.E.T., McCabe, C., 1994. Comparison of magnetic hysteresis parameters of unremagnetized and remagnetized limestones. J. Geophys. Res. 99 (B3), 4613–4623.

Dearing, J.A., Dann, R.J.L., Hay, K., Lees, J.A., Loveland, P.J., Maher, B.A., O'Grady, K., 1996. Frequency-dependent susceptibility measurements of environmental materials. Geophys. J. Int. 124 (1), 228–240.

Dunlop, D.J., 2002a. Theory and application of the Day plot (Mrs/M s versus Hcr/Hc) 1. Theoretical curves and tests using titanomagnetite data. J. Geophys. Res. 107 (B3), 2056.

Dunlop, D.J., 2002b. Theory and application of the Day plot (Mrs/Ms versus Hcr/Hc) 2. Application to data for rocks, sediments, and soils. J. Geophys. Res. 107 (B3), 2057.

Evans, M.A., Lewchuk, M.T., Elmore, R.D., 2003. Strain partitioning of deformation mechanisms in limestones: examining the relationship of strain and anisotropy of magnetic susceptibility (AMS). J. Struct. Geol. 25, 1525–1549.

Fazzito, S.Y., Rapalini, A.E., 2016. Magnetic properties of the remagnetized Middle-Ordovician limestones of the Ponón Trehué Formation (San Rafael Block, Central-Western Argentina): insights into the Permian widespread Sanrafaelic overprint. J. South Am. Earth Sci. 70, 279–297.

Font, E., Trindade, R.I.F., Nédélec, A., 2006. Remagnetization in bituminous limestones of the Neoproterozoic Araras Group (Amazon craton): hydrocarbon maturation, burial diagenesis, or both? J. Geophys. Res. 111 (B06204).

Font, E., Neto, C.F.P., Ernesto, M., 2011a. Paleomagnetism and rock magnetism of the Neoproterozoic Itajaí Basin of the Rio de la Plata craton (Brazil): Cambrian to Cretaceous widespread remagnetizations of South America. Gondwana Res. 20 (4), 782–797.

Font, E., Youbi, N., Fernandes, S., El Hachimi, H., Kratinová, Z., Hamim, Y., 2011b. Revisiting the magnetostratigraphy of the Central atlantic magmatic province (CAMP) in Morocco. Earth Planet. Sci. Lett. 309 (3–4), 302–317.

Font, E., Rapalini, A.E., Tomezzoli, R.N., Trindade, R.I.F., Tohver, E., 2012. Episodic remagnetizations related to tectonic events and their consequences for the South America polar wander path. In: Elmore, R. D. Muxworthy, A. R. Aldana, M. M. Mena, M. (Eds.), Remagnetization and Chemical Alteration of Sedimentary Rocks Geol. Soc. Lond. Spec. Publ. 371, 55–87.

Gómez, F.J., Astini, R.A., 2005. Cianobacterias renalciformes en el Cámbrico Medio de la Precordillera Argentina: morfología, posición estratigráfica y significado

paleoambiental. Ameghiniana 42 (1), 221–232.
Gómez, F.J., Astini, R.A., 2006. Sedimentología y paleoambientes de la Formación La Laja (Cámbrico), Quebrada La Laja, Sierra Chica de Zonda, San Juan, Argentina. Andean Geol. 33 (1), 19–46.
Hrouda, F., Chlupáčová, M., Mrázová, Š., 2006a. Low-field variation of magnetic susceptibility as a tool for magnetic mineralogy of rocks. Phys. Earth Planet. Inter 154 (3–4), 323–336.
Hrouda, F., Chlupáčová, M., Pokorný, J., 2006b. Low-field variation of magnetic susceptibility measured by the KLY-4S Kappabridge and KLF-4A magnetic susceptibility meter: accuracy and interpretational programme. Stud. Geophys. Geod. 50 (2), 283–299.
Ihmlé, P.F., Hirt, A.M., Lowrie, W., Dietrich, D., 1989. Inverse magnetic fabric in deformed limestones of the Morcles Nappe, Switzerland. Geophys. Res. Lett. 16 (12), 1383–1386.
Jackson, M., 1990a. Diagenetic sources of stable remanence in remagnetized paleozoic cratonic carbonates: a rock magnetic study. J. Geophys. Res. 95 (B3), 2753–2761.
Jackson, M., 1990b. Magnetic anisotropy of the Trenton limestone revisited. Geophys. Res. Lett. 17 (8), 1121–1124.
Jackson, M., Craddock, J.P., Ballard, M., Van der Voo, R., McCabe, C., 1989. Anhysteretic remanent magnetic anisotropy and calcite strains in Devonian carbonates from the Appalachian Plateau, New York. Tectonophysics 161, 43–53.
Jackson, M., Rochette, P., Fillion, G., Banerjee, S., Marvin, J., 1993. Rock magnetism of remagnetized Paleozoic carbonates: low-temperature behavior and susceptibility characteristics. J. Geophys. Res. 98, 6217–6225.
Jelínek, V., 1978. Statistical processing of anisotropy of magnetic susceptibility measured on groups of specimens. Stud. Geoph. Geod. 22 (1), 50–62.
Johnson, H.P., Lowrie, W., Kent, D.V., 1975. Stability of anhysteretic remanent magnetization in fine and coarse magnetite and maghemite particles. Geophys. J. Int. 41 (1), 1–10.
Jordan, T.E., Isacks, B.L., Allmendinger, R.W., Brewer, J.A., Ramos, V.A., Ando, C.J., 1983. Andean tectonics related to geometry of the subducted Nazca plate. Geol. Soc. Am. Bull. 94, 341–361.
Katz, B., Elmore, R.D., Cogoini, M., Engel, M.H., Ferry, S., 2000. Associations between burial diagenesis of smectite, chemical remagnetization, and magnetite authigenesis in the Vocontian trough, SE France. J. Geophys. Res. 105, 851–868.
Keller, M., Cañas, O., Lehnert, O., Vaccari, N.E., 1994. The upper cambrian and lower ordovician of the Precordillera (Western Argentina): some stratigraphic reconsiderations. Newsl. Stratigr. 31 (2), 115–132.
Kodama, K., 2012. Paleomagnetism of Sedimentary Rocks: Process and Interpretation, first ed. Blackwell Publishing Ltd., pp. 66–80
Kruiver, P.P., Dekkers, M.J., Heslop, D., 2001. Quantification of magnetic coercivity components by the analysis of acquisition curves of isothermal remanent magnetization. Earth Planet. Sci. Lett. 189, 269–276.
Lowrie, W., 1990. Identification of ferromagnetic minerals in a rock by coercivity and unblocking temperature properties. Geophys. Res. Lett. 17 (2), 159–162.
Lowrie, W., Heller, F., 1982. Magnetic properties of marine limestones. Rev. Geophys. Space Phys. 20 (2), 171–192.
Lu, G., McCabe, C., 1993. Magnetic fabric determined from ARM and IRM anisotropies in Paleozoic carbonates. South. Appalach. Basin. Geophys. Res. Lett. 20 (11), 1099–1102.
Mardia, K.V., 1972. Statistics of Directional Data. Academic Press, London, p. 357.
Milana, J., Zambrano, J., 1996. La cerrillada pedemontana mendocina: un sistema geológico retrocorrido en vías de desarrollo. Rev. Asoc. Geol. Arg. 51, 289–303.
McCabe, C., Jackson, M., Ellwood, B.B., 1985. Magnetic anisotropy in the Trenton limestone: results of a new technique, anisotropy of anhysteretic susceptibility. Geophys. Res. Lett. 12 (6), 333–336.
Oliver, J., 1986. Fluids expelled tectonically from orogenic belts: their role in hydrocarbon migration and other geologic phenomena. Geology 14, 99–102.
Ortiz, A., Zambrano, J.J., 1981. La provincia geológica de Precordillera. In: 8° Congreso Geológico Argentino, San Luis, Actas, vol. 3, pp. 59–74.
Peters, C., Dekkers, M.J., 2003. Selected room temperature magnetic parameters as a function of mineralogy, concentration and grain size. Phys. Chem. Earth 2, 659–667.
Pratt, B.R., Raviolo, M.M., Bordonaro, O.L., 2011. Carbonate platform dominated by peloidal sands: lower ordovician La Silla Formation of the Eastern Precordillera, San Juan, Argentina. Sedimentology 59, 843–866.
Ramos, V.A., 1995. Sudamérica: un mosaico de continentes y océanos. Cienc. Hoy 6, 24–29.
Ramos, V.A., Dallmeyer, R.D., Vujovich, G., 1998. Time constraints on the early palaeozoic docking of the Precordillera, Central Argentina. Geol. Soc. Lond 142 (1), 143–158. Special Publications.
Ramos, V.A., 2004. Cuyania, an exotic block to Gondwana: review of a historical success and the present problems. Gondwana Res. 7 (4), 1009–1026.
Ramos, V.A., Folguera, A., 2009. Andean flat-slab subduction through time. In: Murphy, J.B., Keppie, J.D., Hyenes, A.J. (Eds.), Ancient Orogens and Modern Analogues, vol. 327. Geological Society, London, Special Publications, pp. 31–54.
Rapalini, A.E., 2012. Paleomagnetic evidence for the origin of the Argentine Precordillera, fifteen years later: what is new, what has changed, what is still valid? Latinmag Lett. 2 (1). LL12–0102Rv, 1-20.
Rapalini, A., Astini, R., 1998. Paleomagnetic confirmation of the Laurentian origin of the Argentine Precordillera. Earth Planet. Sci. Lett. 155 (1–2), 1–14.
Rapalini, A.E., Bordonaro, O., Berquo, T.S., 2000. Paleomagnetic study of Cambrian-Ordovician rocks in the Eastern Precordillera of Argentina: some constraints on the Andean uplift of this block. Tectonophysics 326 (1–2), 173–184.
Rapalini, A.E., Cingolani, C.A., 2004. First late Ordovician paleomagnetic pole for the Cuyania (Precordillera) terrane of Western Argentina: a microcontinent or a Laurentian plateau. Gondwana Res. 7 (4), 1089–1104.
Rapalini, A.E., Astini, R.A., 2005. La remagnetización sanrafaélica de la Precordillera en el Pérmico: nuevas evidencias. Rev. Asoc. Geol. Argent. 60 (2), 290–300.
Raviolo, M.M., Bordonaro, O.L., Pratt, B.R., 2007. Revisión estratigráfica y litofacial de la Formación La Silla (Ordovícico Inferior) en la Precordillera Oriental de San Juan, Argentina. Lat. Am. J. Sed. Basin Anal. 14 (2), 117–128.
Raviolo, M.M., Barbosa, J.A., Neumann, V.H., 2009. Characteristics, distribution and diagenetic stages of chert in the La Silla Formation (lower ordovician), Argentine Precordillera. Ann. Braz. Acad. Sci. 81 (4), 781–792.
Rochette, P., Jackson, M., Aubourg, C., 1992. Rock magnetism and the interpretation of magnetic Susceptibility. Rev. Geophys. 30 (3), 209–226.
Schmidt, V., Günther, D., Hirt, A.M., 2006. Magnetic anisotropy of calcite at room-temperature. Tectonophysics 418 (1–2), 63–73.
Symons, D.T.A., Cioppa, M.T., 2000. Crossover plots: a useful method for plotting SIRM data in paleomagnetism. Geophys. Res. Lett. 27 (12), 1779–1782.
Tarling, D.H., Hrouda, F., 1993. The Magnetic Anisotropy of Rocks. Chapman and Hall, London, p. 217.
Thomas, W.A., Tucker, R.D., Astini, R.A., 2000. Rifting of the Argentine Precordillera from Southern Laurentia: palinspastic restoration of basement provinces. Geol. Soc. Am., Abstr. Programs 32, A-505.
Trindade, R.I.F., D'Agrella-Filho, M.S., Babinski, M., Font, E., Brito Neves, B.B., 2004. Paleomagnetism and geochronology of the Bebedouro cap carbonate: evidence for continental-scale Cambrian remagnetization in the São Francisco craton. Braz. Precambrian Res. 128 (1–2), 83–103.
Truco, S., Rapalini, A.E., 1996. New evidence of a widespread Permian remagnetizing event in the Central Andean zone of Argentina. Third International Symposium on Andean Geodynamics, St. Malo, Extended Abstracts, 799–802.
Vergés, J., Ramos, V.A., Meigs, A., Cristallini, E., Bettini, F.H., Cortés, J.M., 2007. Crustal wedging triggering recent deformation in the Andean thrust front between 31°S and 33°S: sierras Pampeanas-Precordillera interaction. J. Geophys. Res. 112 (B03S15).
von Gosen, W., 1992. Structural evolution of the Argentine Precordillera: the Rio San Juan section. J. Struct. Geol. 14 (6), 643–667.
Zapata, T.R., Allmendinger, R.W., 1996. Growth stratal records of instantaneous and progressive limb rotation in the Precordillera thrust belt and Bermejo basin, Argentina. Tectonics 15 (5), 1065–1083.
Zegers, T.E., Dekkers, M.J., Bailly, S., 2003. Late carboniferous to permian remagnetization of devonian limestones in the ardennes: role of temperature, fluids, and deformation. J. Geophys. Res. 108 (B7), 19.